Delft University of Technology
Master's Thesis in Embedded Systems

Relative Localization for Mobile Nodes using Visible Light

Aniruddha Deshpande

Relative Localization for Mobile Nodes using Visible Light

Master's Thesis in Embedded Systems

Embedded Software Section
Faculty of Electrical Engineering, Mathematics and Computer Science
Delft University of Technology
Mekelweg 4, 2628 CD Delft, The Netherlands

Aniruddha Deshpande
a.deshpande@student.tudelft.nl

23rd September 2016

Author
Aniruddha Deshpande (a.deshpande@student.tudelft.nl)
Title
Relative Localization for Mobile Nodes using Visible Light
MSc presentation
30th September 2016

Graduation Committee

Prof. dr. K.G. Langendoen (chair)	Delft University of Technology
Asst. Prof. dr. M.A. Zuniga Zamalloa	Delft University of Technology
Assoc. Prof. dr. Johan Pouwelse	Delft University of Technology

Abstract

A growing number of wireless devices and increasing traffic in the radio spectrum has pushed for alternatives to radio based communication. Among these, communication using visible light (VLC) has gained considerable momentum. The imminent adoption of energy efficient Light Emitting Diodes (LEDs) and the high data transmission rates offered by VLC has greatly contributed to the spread of visible light as a competitive communication medium. Apart from communication, another area greatly benefiting from visible light is localization. A significant amount of work has been done in localization for VLC based networks, however most of the methods proposed are dependent on either surrounding environments or require multiple reference points at *fixed* positions for localization. These dependencies greatly restrict localization for scenarios where a lot of mobility is involved, such as vehicles on a road, or robots in an industrial environment.

This master thesis presents a localization model which can be used to find the relative position of devices or nodes without such dependencies. Compared to the existing work in this field, in our proposed model, nodes are free to move and rotate in any direction, and only require a single light source for position estimation. We present a mathematical model for relative localization and a software implementation to visualize the location of nodes in real-time. Results from experiments conducted in both static and mobile settings under different illumination levels validate our proposed model. These results also highlight the effect of errors in received power and orientation of nodes on localization accuracy. Our work indicates that this proposed model can be further extended and implemented in a real world scenario.

Preface

This thesis describes the work done by me during the past 8 months, for a Master of Science in Embedded Systems at Delft University of Technology. I was drawn towards computers from an early age, and over the course of my education, my interest in them has only grown, especially in the domain of embedded systems. Small, computing devices which can communicate with each other, and interact with their environment became the focus of my studies during the past two years. Recently, improvements in technology have made it possible that these devices can now communicate using visible light, which I find to be truly fascinating. I was always inclined towards the field of optics, and choosing visible light communication as a domain for my thesis, has helped me learn more about it than I could have ever imagined. During the course of my studies, I was also introduced to the concept of localization, and learnt about various scenarios where it can be applied. This work describes one such scenario, where localization can be done using visible light. Working on this thesis was not only interesting, but also challenging, which has made it a memorable experience.

I wish to express my deepest gratitude, to Marco Zuniga, for introducing me to the field of visible light communication and localization. This work couldn't have been realized without his generous support and necessary critique. His guidance was crucial for this thesis, and his knowledge and experience have helped me greatly with my writing and presentation skills. I am also glad that I could be a part of the 'VLC Power Group' meetings with Marco, Jake and Johnny. These meetings taught me a lot about critical thinking, and also helped me learn more about Peruvian, Chinese and Dutch cultures. My education and work here in the Netherlands couldn't have been possible without the help of two wonderful people, Aditya and Geeta. I will be forever grateful to both of you. Lastly, I would like to thank my parents, who have been with me through all the times, and given me their unconditional love and support.

Aniruddha Deshpande

Delft, The Netherlands
23rd September 2016

Contents

Chapter 1

Introduction

Wireless communication has become an integral part of our day to day lives. Using radio waves or radio frequency (RF) has been the standard for wireless communication for decades now. From the first wireless telegraphy system developed by Guglielmo Marconi in 1894 to the widespread cellular and satellite communications of today, wireless communication has advanced and has been adopted at a tremendous rate. In the information age of today, wireless devices in the form of cellphones and laptop computers can be found everywhere. In addition to this, applications for Internet of Things have grown mainly due to the advent of devices like smart TVs and smart lights. However, the growth of wireless devices at our homes and workplaces comes at a cost. With RF being the standard wireless medium, the available bandwidth for radio communication is steadily decreasing. This has pushed research for alternative forms of communication which utilize different regions of the electromagnetic spectrum such as microwave, infra-red, and even visible light.

Communication using Visible Light (VLC) has been gaining momentum in the past few years but it is not a new concept. It was adopted in the eighteenth century by ships at sea, which used gas lanterns with shutters to send short messages. This was later replaced by radio, which was faster and could offer better communication over long distances. Now, some experimental forms of VLC can offer data transmission speeds reaching as high as a few gigabits per second, which is well beyond the speeds offered by conventional RF. Recent work by Disney research, also shows the wide range of VLC applications in toys. However, VLC is not meant to replace RF, at least in the near future, but instead aims to provide a communication framework over the existing lighting infrastructure.

Devices which communicate using visible light can also form networks of their own, and like any other wireless network, they also offer an opportunity for localization. *Localization refers to determining the location or position of a person or an object.* This information about the position of a device in a wireless network, can be greatly useful in providing location based services and opens a window for a variety of applications. Some applications for localization can include providing navigation for users in large indoor areas such as airports, tracking/locating robots in industrial environments, or even vehicle-to-vehicle relative localization. Visible Light can also be used for localization.

A considerable amount of work has been done in using visible light for positioning, but it usually involves indoor scenarios in static environments. The localization of an object or a user in most of these studies is done with reference to a single or multiple fixed points. There is a need for localization methods in dynamic or mobile scenarios. Examples of such scenarios can be vehicles on a road or even industrial robots which need to be mobile in harsh environments. These vehicles or robots can use their on-board lights to communicate with each other and share the changes in their position. There are existing methods based on RF which can be applied to such dynamic scenarios. However, such methods generally involve a trade-off between accuracy, robustness and economic investment. Herein lies *a challenge to implement a localization method which can provide high accuracy positioning in dynamic or mobile scenarios with minimal infrastructure investment.*

This is where localization using VLC can be truly valuable. There are some fundamental properties of light that enable us to provide a high degree of accuracy in positioning. Moreover, these properties can provide us with a *localization method where only a single beacon for reference is sufficient.* Requiring just a single beacon is greatly beneficial especially in mobile scenarios where both the reference and target are free to move, such as vehicles on a road. Add to this an existing lighting infrastructure which includes light fixtures in buildings, street lights and inexpensive light sensors which have already found home in our smart-phones and cars, greatly reduce the initial infrastructure investment. These advantages coupled with the shift towards energy efficient LED lamps, affirm the feasibility of VLC for localization.

1.1 Problem Definition

Even in the realm of Visible Light Communication, localization of objects or *nodes* can be achieved using several methods. A majority of these methods depend on using multiple reference points, or sources of light in this case to calculate the position of an object. Some of these methods might also require information or even a map of the region where localization is to be done. Such requirements for the number of light sources and map/information of the environment can be very restrictive for applications in mobile scenarios.

Consider an example of two *nodes*, where one of them is trying to follow the other. This can also be visualized as two vehicles, like cars or bikes moving on a road. For one node to follow the other, it needs to know its position relative to the other. If these nodes rely on their surroundings to find their location, then:

(a) nodes will be restricted to that environment, or

(b) any change in the environment, for example if reference points are moved or obstructed, could potentially disrupt the system.

In such cases a solution is needed which can describe the relative position of these nodes, without any prior knowledge of their surroundings. To summarize:

Localization of nodes in mobile/dynamic scenarios requires a degree of independence from the environment and a minimum possible number of reference points.

It is also required that the localization rely on using the least number of transmitters and receivers to ensure that the nodes can freely move and orient themselves in any direction, while maintaining a communication link between them.

1.2 Thesis Contribution

The contributions of this thesis can be described as follows:

- We propose a model for localization using visible light which can be used to calculate the position of nodes in both static and mobile scenarios. The model can describe the position of a node which can move freely and rotate in any direction using only a single beacon as a reference also under different illumination levels. In case of mobile scenarios, both the reference node and the target node to be localized have the freedom to change their position and orientation.
- We provide a software implementation of our localization method which uses a combination of the OpenVLC cape, a BeagleBone and orientation sensors to provide a visual representation of node positions in real-time. In addition to this, implementing communication as a part of localization is also discussed.
- We evaluate the implementation of the proposed model for a scaled down system and analyse the performance for two scenarios, static and dynamic. We also analyse the factors which affect the accuracy and robustness of this localization model.

1.3 Structure and Organization

In the upcoming chapter, we get an overview of VLC, the different types of transmitters and receivers required for visible light and the different modulation schemes used in communication. The following Chapter 3, describes the proposed localization model by first explaining the system, the prerequisites required for localization and finally the localization method. Chapter 4 elaborates on the implementation specifics, such as the hardware and software setup, and how localization can be achieved while communicating with visible light. The results and evaluation chapter discusses in detail the results obtained for two cases, static and dynamic scenarios and the factors which affect the accuracy of the model. Lastly, the conclusion is presented in Chapter 6.

Chapter 2

Background

Communication using visible light is also known as *LiFi*. It finds its place in the Internet of Things, and has also been proposed as a component in the context of communication and data broadcasting. With the increasing RF-bandwidth limitations, it is not difficult to conceive a house or an office building, which can leverage its existing lighting infrastructure to provide a communication framework. Such a framework would involve a network of lights, which can communicate and share information with each other and thus, could in turn establish an Internet of Lights.

Data transmission essentially involves modulation of the carrier medium, which in this case can be switching a light source on and off. There are also more intricate modulation schemes described for this purpose in the IEEE 802.15.7 protocol [15]. Localization can be an integral part of light based networks, and there are several ways to do localization using visible light, many of which are based on the ones used in RF networks [12], [13]. These can include methods based on using multiple reference points to get a position estimate or even mapping how light intensity is distributed in a region.

2.1 Communication using Visible Light

The transmitters and receivers in VLC can be quite different from the traditional ones of RF communication where an antenna plays both roles. VLC usually involves data transmission using LEDs and reception using devices sensitive to light. LEDs can be switched on and off, where an *on* state can imply logic high, and on *off* state could mean a logic low. This type of data transmission can be illustrated in Figure 2.1.

2.1.1 Transmitters and Receivers

Transmitters

VLC or LiFi uses light-emitting diodes (LEDs) as a medium to transmit information. Semiconductor based LEDs have a unique property that they can be switched ON and

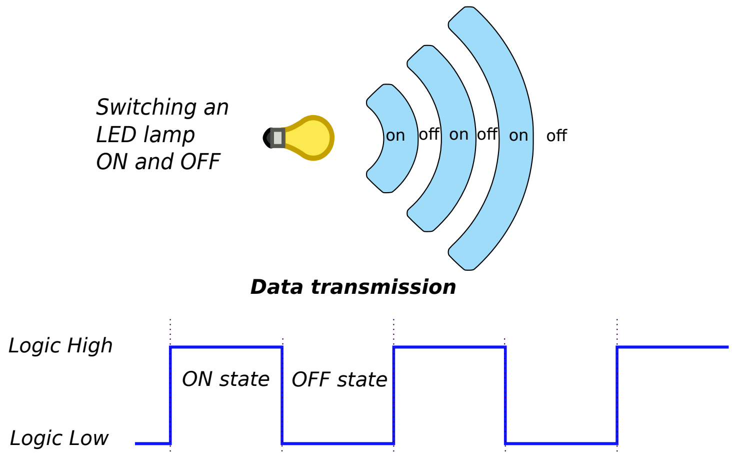

Figure 2.1: Data transmission in VLC by switching LED states.

OFF really fast. One concern is that this switching might be seen as flickering, which can be annoying. But, because of the semiconductor properties of an LED, this state change can be fast enough that it is invisible to the human eye, giving an illusion that the lamp is in a constant ON state.

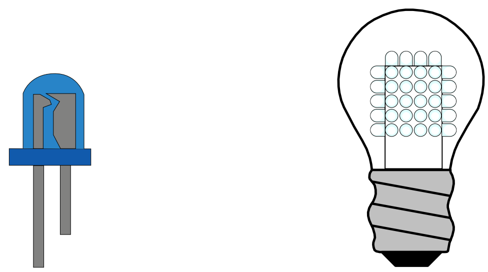

Figure 2.2: An LED and an LED lamp which can be used for visible light communication.

Receivers

The receivers for visible light communication need to detect the on and off state changes of the transmitting light source. This can be done using devices which are sensitive to light, such as a photodiode, or even an image sensor used in cameras. The most commonly used receivers in light based communication are as follows:

(i) **Photodiode**
A photodiode is a device which produces current when light is incident on it. When

modulated light falls on a photodiode, the current produced fluctuates corresponding to the modulation, i.e., the current produced would increase during the on state of the transmitter and decrease during the off state. These fluctuations can be used to define logical states of high and low, which in turn can be interpreted as binary data. Figure 2.3 illustrates the spectral responsivity of a photodiode with respect to different wavelengths of light. Although these devices are fairly inexpensive, using them requires dedicated circuitory for amplifying the signal and reducing noise.

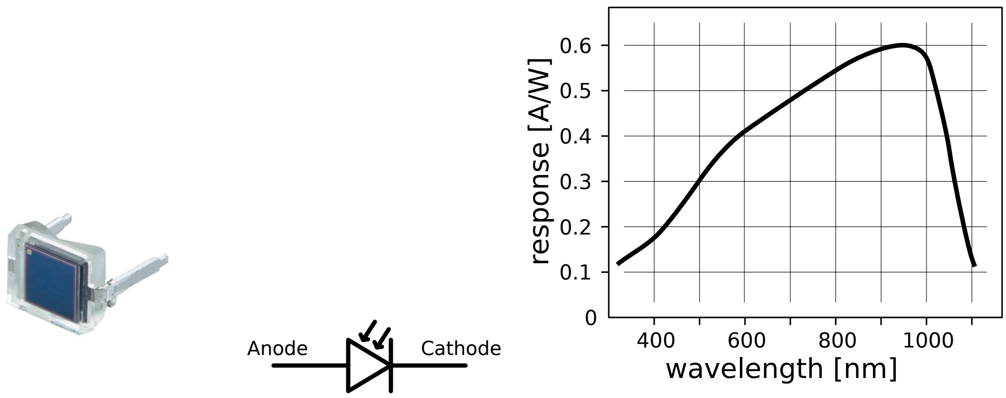

Figure 2.3: A Photodiode, its symbol and response to incident light of different wavelengths [21].

(ii) **Image Sensors**

Image sensors can also be used as receivers for visible light communication. However these sensors work differently than photodiodes. Such sensors are usually Complementary Metal-Oxide Semiconductor (CMOS) sensors and are readily available in almost all smartphones today. One way to decode VLC data using CMOS sensors is to process the image frames recorded by the sensor where one or a couple of frames could represent a data bit. However, the data transmission rate in this case is restricted by the frame-rate of the sensor which is quite low at around 30fps.

An alternative method to decode information uses the *rolling shutter effect* [7]. When capturing an image, instead of exposing all the pixels in a CMOS sensor, which is known as a *global shutter*, each row of pixels, is exposed one after the other. As each row is exposed at a different moment in time, images for fast moving objects can appear distorted. However, when modulated light is captured using this rolling shutter effect, the resulting image can capture the modulation in the form of dark and light bands. These bands as shown in Figure 2.4 represent binary data, which can be decoded. Using the rolling shutter effect for decoding is much faster as a single frame can now consist of multiple data bits instead of one frame being used to represent a single bit.

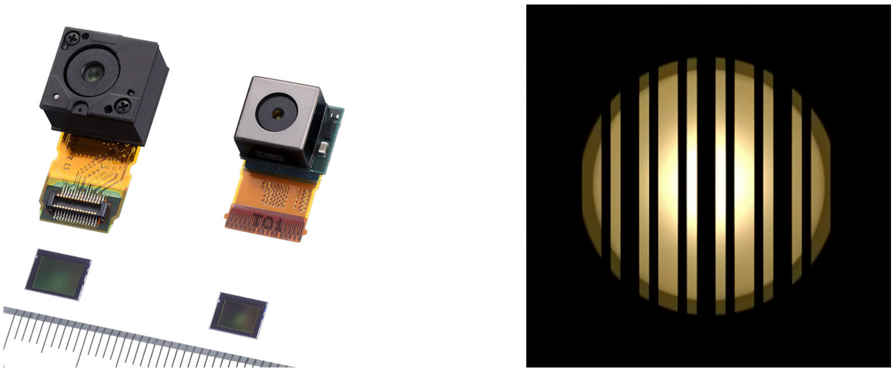

Figure 2.4: Image sensors and the Rolling shutter effect with dark and light bands.

The primary disadvantage of using image sensors is their cost. CMOS sensors are usually paired with complex hardware behind them which is required to process the images recorded in order to process data. Also, the data transmission rates achieved by using these sensors is also very low compared to photodiode based receivers.

(iii) **Light Emitting Diodes**
LEDs are usually used for transmitting light, which happens when electrons flow in the semiconductor material to produce photons. The reverse of this is true for photodiodes, where incident photons can lead to a flow of electrons. With little change in the circuit i.e., connecting an LED in reverse bias mode, it can be made to behave as a photodiode, consequently acting as a receiver. However, LEDs are not very good receivers when compared to photodiodes, because they are relatively less sensitive and also have a limited field of view due to their shape and size.

For this project, we use LEDs as transmitters because of their cost, power efficiency and most importantly, their ability to switch on and of really fast. On the receiver side, photodiodes are used, due to their simplicity, cost and ability to proved high data transmission rates.

2.1.2 Modulation Schemes in Visible Light Communication

Light can be modulated in several ways to encode and transmit data. Different modulation schemes, have different advantages as some provide robustness and range, while there are others with high data transmission rates. These modulations can be based on amplitude, frequency or even color of the light medium [15]. Some of the relevant modulation schemes are described below:

- **Amplitude based modulation**: Amplitude modulation for visible light is very similar to the modulation in radio signals, but is more commonly referred as intensity modulation. The most simple scheme for this can be *On-Off keying.* In this modulation scheme, the carrier signal is turned on or off for a particular duration of time. This type of modulation is the most convenient to implement, however it is also very sensitive to noise. Other forms of modulation include, *Pulse position or Pulse width modulation.* Such schemes are based on modifying the ratio between the on and off times of the light signal

- **Frequency based modulation**: Frequency based modulation is quite different from the conventional methods in radio. Unlike radio, changing either the phase or frequency of light is rather difficult. Instead, the modulation looks quite similar to On-Off keying, except rather than just turning the light medium on or off, the frequency of this switching is changed.

- **Color based modulation** Another form of modulation is based on the color of the light medium. Recent work done in this area has produced modulation schemes such as *Color Intensity Modulation* and *Color Shift Keying* with data transmission rates as high as 96Mbps [14].

There are many other sophisticated modulation schemes which have greatly increased the data transmission rates such as *Orthogonal Frequency Division Multiplexing* (OFDM) [4] or *Quadrature Amplitude Modulation* (QAM) [18], but in this research project we choose On-Off keying because of its simplicity and ease of implementation.

2.2 Related work

There is a huge amount of work done in the field of localization using radio waves. The work done involves different forms of radio waves such as wide-band, ultra wide-band even microwave, and methods which can be used in a vast number of scenarios providing different levels of accuracy [12]. In the past few years, the research for localization using visible light has also picked up pace. Many of the techniques for localization using light are greatly influenced from the pre-existing methods based on radio waves [13]. However, now many localization methods have been proposed which not only build on existing RF techniques, but also exploit the unique properties of light [8].

2.2.1 Methods inherited from RF

As described in [12], there are a number of ways to determine the position of an object using radio waves. The same methods could be applied for visible light. Broadly, these methods can be grouped together in the following categories:

(i) **Proximity based methods**

One of the most simplest location estimation techniques is based in *Proximity*. This method can be used to derive the approximate position of a user or an object based on its proximity from a base station.

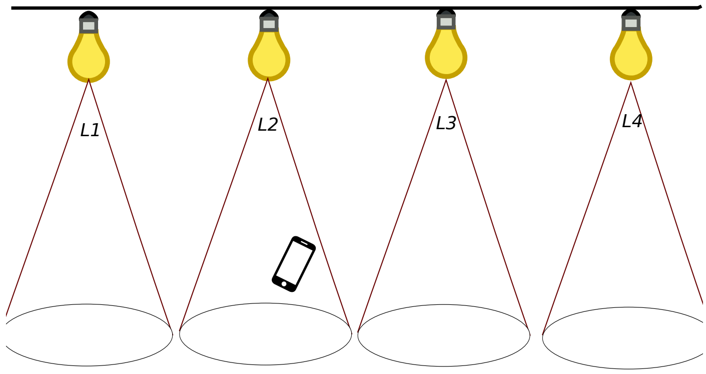

Figure 2.5: Proximity based estimation using light sources with unique IDs.

The system for such a localization would involve the installation of a dense grid of lights on the ceiling, where each light source could transmit its own unique identification. A device such as a smartphone equipped with a photodiode could receive this communication from overhead light sources to identify them from their unique identifications. Using this, the position of the user or an object can be determined as the location of the light source which has the strongest signal.

Proximity based methods do not offer a very high accuracy for localization. The accuracy of the position estimate in case of proximity based systems is directly dependant on the number of light sources installed. However because they are easy to implement and simple to understand, they are useful for a number of applications. A system to locate wheelchairs and medical equipment for a hospital is proposed in [6].

(ii) **Fingerprinting or Scene Analysis**

Another method for localization is based on *Fingerprinting* or *Scene analysis*. This method consists of two phases, an offline phase and an online phase. The offline phase involves mapping and recording location related data. Location related data usually refers to the received signal strength or the distribution of light intensity. In the offline phase this intensity distribution along with an ID of the light source is recorded for all the possible places in an environment. During the online phase, measured data is matched against this pre-recorded dataset to determine the position.

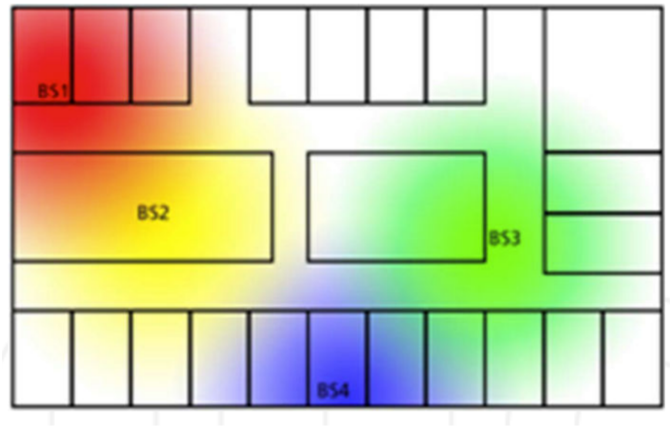

Figure 2.6: A map of light intensity distribution in an indoor environment.

There are many approaches to scene analysis with differences mainly in the algorithms used during the online phase. Localization is achieved with the help of algorithms based on pattern recognition including correlation, probabilistic methods and k-nearest neighbour (kNN). A probabilistic method based on the Bayesian model is proposed in [9], which showed robustness to disturbances such as light reflection and obstructions. An accuracy of $0.81m$ was achieved in the simulation for an area of $30 \times 30m^2$.

Another frequently opted method uses the $k-$Nearest Neighbour (kNN) algorithm. Based on the measurement done in the online phase, kNN can be used to determine the distance between the offline signal strength vector and the online signal strength vector. Once this distance is calculated with respect to all possible locations, the ones with the shortest distance are chosen as the location. [17] describes an experiment conducted in a room measuring $180 \times 120cm^2$, where the distance between location candidates itself was $10cm$. The position estimate in this case had an average distance error ranging from $15cm$ to $20cm$.

Scene analysis can be accurate, however there a re instances when it is not very effective. These methods are prone to noise from external sources like windows, reflective materials and have a tendency to report multiple locations. There also some cases, where due to the lighting configuration, large areas can have the same light intensity.

(iii) **Triangulation or Trilateration**
Arguably, of all the localization methods inherited from RF, triangulation based methods have attracted the most amount of research. This is mostly because, these methods can, at least theoretically, provide the absolute position of a user or an object instead of the position estimates discussed in the previous methods. There are many different ways to perform triangulation, which can be divided into

angulation methods and *lateration* methods. Lateration based methods rely on calculating the distances between a mobile node and multiple light sources. This distance estimation can be done in several ways, such as calculating the time it takes for a signal to arrive or how much the signal attenuates.

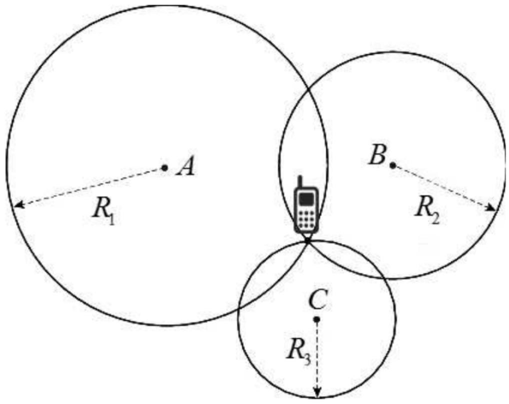

Figure 2.7: 2-D Trilateration based on distance estimation.

Distance estimation can also be achieved by measuring channel attenuation. A positioning system, *Epsilon* [11], used multiple light sources as reference for localizing a smartphone equipped with a photo-sensor. Varying accuracy ranging from $0.4m$ to $0.8m$ was recorded in different office environments for this system. However, this method involves the smartphone to be rotated by the user in a particular way to determine the location.

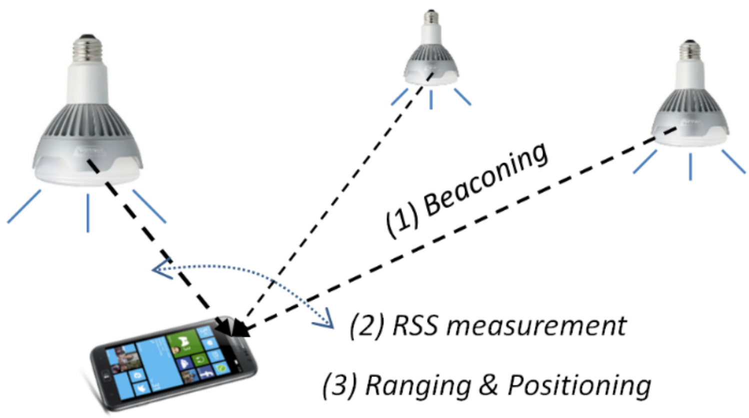

Figure 2.8: Smartphone localization based on channel attenuation. *Epsilon*[11].

Time of Arrival (TOA) is one such method which calculates the distance between a mobile device and a light source by measuring the arrival time of signals. These distances are used to trilaterate the exact position of the mobile node.

However, this method requires measuring the arrival time of signals, time-keeping especially for light can be really complex and difficult. Also this means, that all devices on the network must have their clocks synchronized to a very high degree of accuracy. One alternative to this problem uses the *Time Difference of Arrival* (TDOA) where the difference in the arrival times of signals is considered. An application of TDOA can be seen in an automotive use case as described in [16], where relative localization was proposed using two pairs of transmitters and receivers each, corresponding to the head and tail lights of vehicles. This difference can be used to estimate the distance from the light sources, however multiple reference points and transmitter synchronization are still needed for localization.

Angulation methods are based on deriving the angle relative to multiple reference points. Multiple light sources are used to determine the position of a mobile device by calculating the angle of arrival (AOA) of signals. The calculated angles provide multiple bearings as shown in Figure 2.9. At the intersection of these bearings, a mobile device can be located.

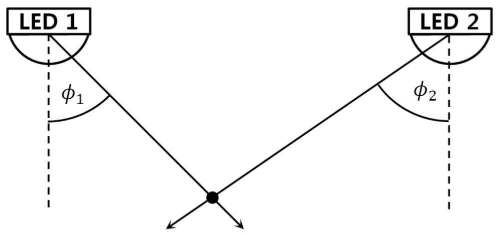

Figure 2.9: Localization using angle of arrival from multiple LEDs

AOA for light is much more advantageous than AOA for radio waves as light is inherently directional and the signal transmitted is in Line of Sight (LOS). Also unlike radio, light sources don't require an array of antennas for directional transmission. AOA methods involve multiple reference points, but in some cases a combination of multiple transmitters and receivers can also be used for localization. In [5], a combination of three orthogonal photodiodes was used along with multiple LED sources. Because of their placement, different photodiodes measured different signal strengths. Simulation results showed that positioning error could be reduced to $5cm$.

Similar work has been done in the positioning system *Luxapose* [10]. In this work, instead of a photodiode, a CMOS sensor is used as a receiver. Rolling shutter effect [7] of a camera is used to demodulate the signal transmitted by multiple light sources. However, the CMOS sensor itself is also used as an angle of arrival sensor to provide localization at decimeter level of accuracy.

There are other methods which use a camera sensor and perform image/vision analysis to determine the location of a mobile node. But in this project we only focus on those methods which can be implemented using the simplest of transmitters and receivers such as photodiodes. This provides the advantage of reduced costs and relative ease in implementation of the system.

2.2.2 Methods suited for our system

In this project we propose a localization method which involves both the angle of arrival and the estimation of distance through channel loss. The localization environment involves *mobility*, hence emphasis is given on methods which require the least possible number of reference points and no pre-recorded information regarding the environment.

LiPro [22] is one such method which uses a single pair of transmitter and receiver for localization. The study was published as recently as June 2016 describing localization of a smartphone using a light source fixed on the ceiling. In order to do this the smartphone has to be rotated around three axes, in a way similar to the calibration of a magnetic sensor.

Another localization system proposed by Yin & Haas [24], describes a method which uses both angle of arrival principles and attenuation of light signal to estimate the position of a mobile device. This method extends the proofs presented in [23], and describes a positioning system with multiple photodiodes installed on a ceiling acting as receivers. Localization is done for a mobile device made of multiple LEDs fixed at different angles acting as a transmitter, also known as an *angle diversity transmitter* (ADT). The simulation results presented in the paper, described a decimeter level of accuracy for different configurations of the ADT. The work proposed by Yasir [23] also involves using the lambertian model for localization. In this work, both single or multiple transmitters can be used to localize a receiver. However, transmitters in this case were also stationary.

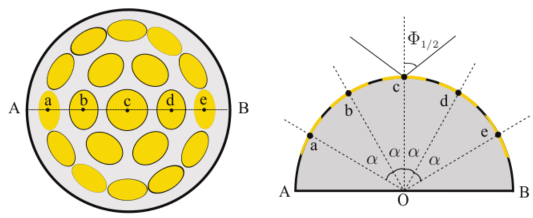

Figure 2.10: Angle diversity transmitter described in [24].

In this project, we build on the work described in [24] and [23], by proposing a localization method which requires only a *single* transmitter and receiver configuration. Moreover, we show that the localization method can be implemented in truly dynamic environments, i.e. *both the transmitter and receiver can be mobile*, by performing tests on a scaled version of the system. The following Table 2.1 can be used to compare different methods with this project.

Table 2.1: Comparing different works with this project

Study	**Receivers**	**Transmitters**	**Analysis**	**User Calibration**	**Mobility**
Lipro [22]	Single Photodiode	Single LED	Empirical	Yes	Static (Transmitter fixed)
Epsilon [11]	Single Photodiode	Multiple LEDs	Empirical	Yes	Static (Transmitter fixed)
Haas [24]	Single Photodiode	Multiple LEDs	Theoretical	No	Static (Receiver fixed)
Yasir [23]	Single Photodiode	Single/Multiple LEDs	Empirical	No	Static (Transmitter fixed)
Luxapose [10]	Single Image Sensor	Multiple LEDs	Empirical	No	Static (Transmitter fixed)
This project	Single Photodiode	Single LED	Empirical	No	Dynamic (Transmitter and receiver can be mobile)

Chapter 3

Model

In this chapter, the system model and the pre-requisites for understanding localization using visible light are outlined. Further, a localization model based on these concepts is proposed.

3.1 System of Mobile Nodes

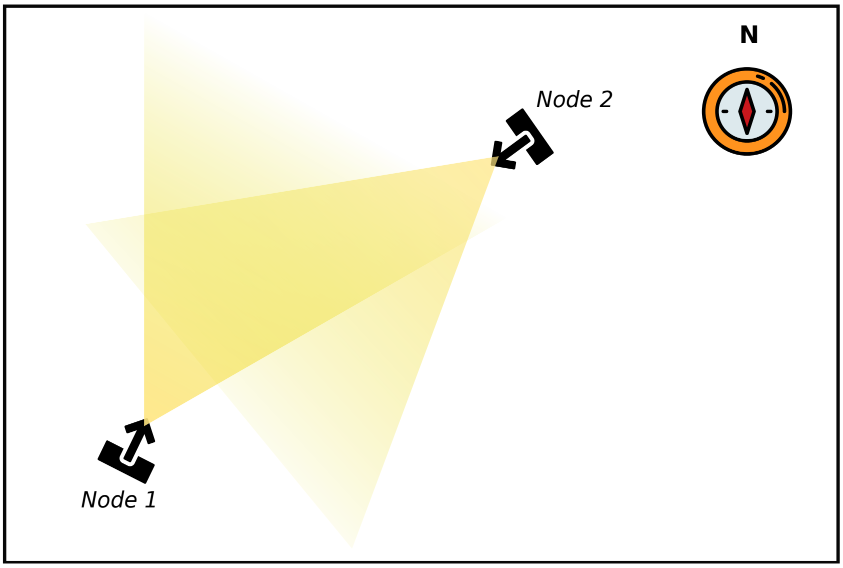

Figure 3.1: A 2-D system of mobile nodes communicating using visible light

Before a localization model can be explained, the system where the model can be applied needs to be defined. Vehicles on a road, such as cars even bicycles, or autonomous robots following each other can be considered as examples of our system. In this project, the system for our localization methods consists of at least 2 *nodes*. These nodes are devices that consist of an LED, a photodiode acting as transmitter and receiver respectively, and an orientation sensor. These nodes have the capability to communicate with each other using visible light. Further, the nodes are *mobile*, i.e. they are free to move and orient themselves in any direction. The only reference these nodes have is their orientation with respect to magnetic north. For this project, a 2-D system of nodes is considered and described in Figure 3.1. The proposed localization method, would help the nodes in this system to obtain their position, relative to each other.

3.2 Understanding Radiation Patterns for Visible Light

The proposed model is based on radiation patterns of visible light. When light is emitted from a source, it forms a pattern. Understanding radiation patterns requires understanding the cosine law, shape of the pattern for different light sources and the attenuation of light with distance. Lambert's cosine law describes how the intensity of light changes within the radiation pattern of a light source. Further, the shape and size of radiation patterns is dependant on characteristics of the light source. Lastly, we outline the factors which contribute to the attenuation of a light signal.

3.2.1 Lambert's Cosine Law

Lambert's cosine law or Lambert's emission law is named after Johann Heinrich Lambert from his work *Photometria* published in 1760, where he first described the concept of perfect diffusion. When light falls on a surface, depending on that surface, it can reflect in two ways. Either it can reflect like a mirror, this is known as *specular reflection*, or it can diffuse in different directions. Such type of reflection is termed as *diffuse reflection*. Any surface which obeys Lambert's law is termed as a *Lambertian*.

Cosine Law -:

> *The radiant intensity or luminous intensity observed from an ideal diffusely reflecting surface or ideal diffuse radiator is directly proportional to the cosine of angle between the direction of the incident light and the surface normal.*

Figure 3.2, illustrates the radiation pattern of a light source. The cosine law can be explained using this figure quite clearly. Consider, the intensity of light measured from a distance at the surface normal to be I. This is also indicated by the region in blue. The cosine law states that, the intensity of light in the region described in red is directly proportional to the cosine of the angle formed between itself and the surface normal.

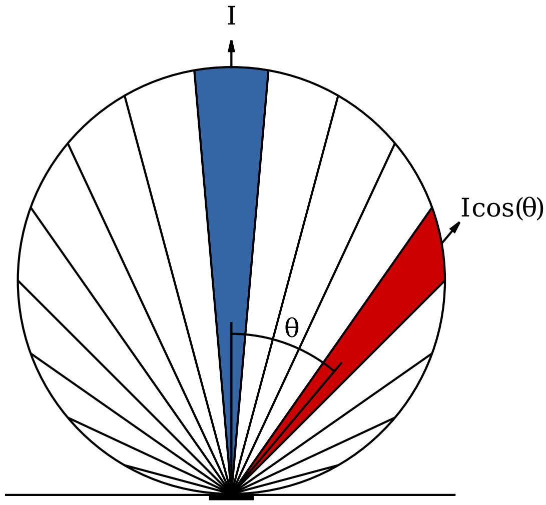

Figure 3.2: Lambert's cosine Law

3.2.2 Radiation patterns for different light sources

Different light sources have their individual optical characteristics which define their radiation patterns. The radiation pattern for a light source is guided by a mathematical order. Mathematically it is termed as the Lambertian order and is denoted by the symbol m. From [25], this order can be defined using the following equation:

$$m = \frac{-ln(2)}{ln(cos(\phi_{1/2}))} \tag{3.1}$$

In equation 3.1, the term $\phi_{1/2}$ is used to describe the semi-angle of an LED at half-power. Or formally, the off-axis point at which the intensity of an LED is half its on-axis intensity is referred to as the LED's *semi-angle* or $\phi_{1/2}$. Figure 3.3 shows how the LED semi-angle can be calculated.

From the equation we can infer that the possible values for this order m can range from 0 to ∞. Figure 3.4 illustrates the difference in the radiation pattern for light sources with differing values of m. The region defined in yellow, describes the radiation pattern for a light source with the lambertian order $m = 1$. Such a pattern is called an ideal lambertian pattern. Light sources with a wide field of view, have a large semi-angle and consequently a very low value for m. This leads to a broad radiation pattern. As the field of view for a light source becomes decreases, so does its semi-angle and consequently, the value of m increases. A large value of m leads to a long and directional radiation pattern. It can be seen from the figure that a light source with a high value of $m = 50$ has a very narrow radiation pattern as depicted by the region in black. Also the intensity of light

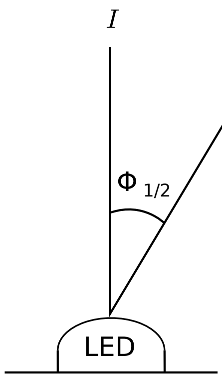

Figure 3.3: Determining the semi-angle for an LED source

in this region should be very high. Figure 3.4 shows radiation patterns with normalized intensity. A key point to note is, that radiation patterns for light are more stable over time compared to the patterns of radio.

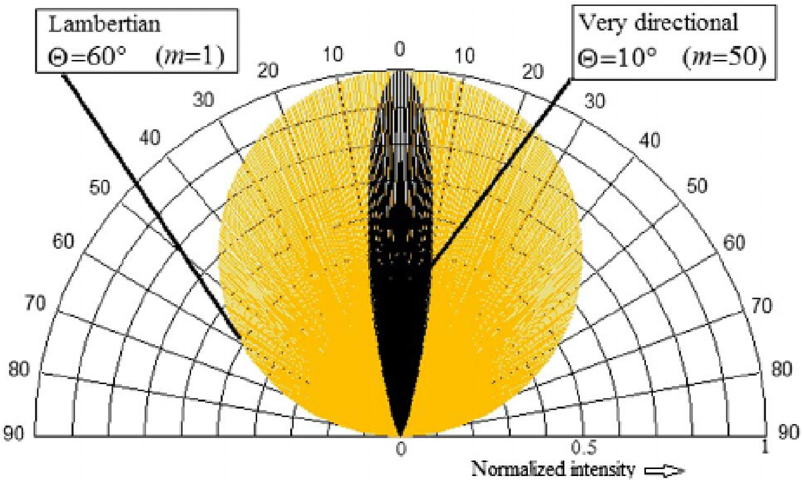

Figure 3.4: Different radiation patterns for varying values of m

3.2.3 Channel loss for visible light

When energy, either in the form of light, radio or any other component of the electromagnetic spectrum is emitted through a transmitter, it suffers through attenuation. From the inverse square law, we know that the intensity for such radiation is inversely proportional to the square of distance [20]. In case of light, this attenuation or decay of signal strength increases with distance and various other factors. This attenuation can be seen in Figure 3.5.

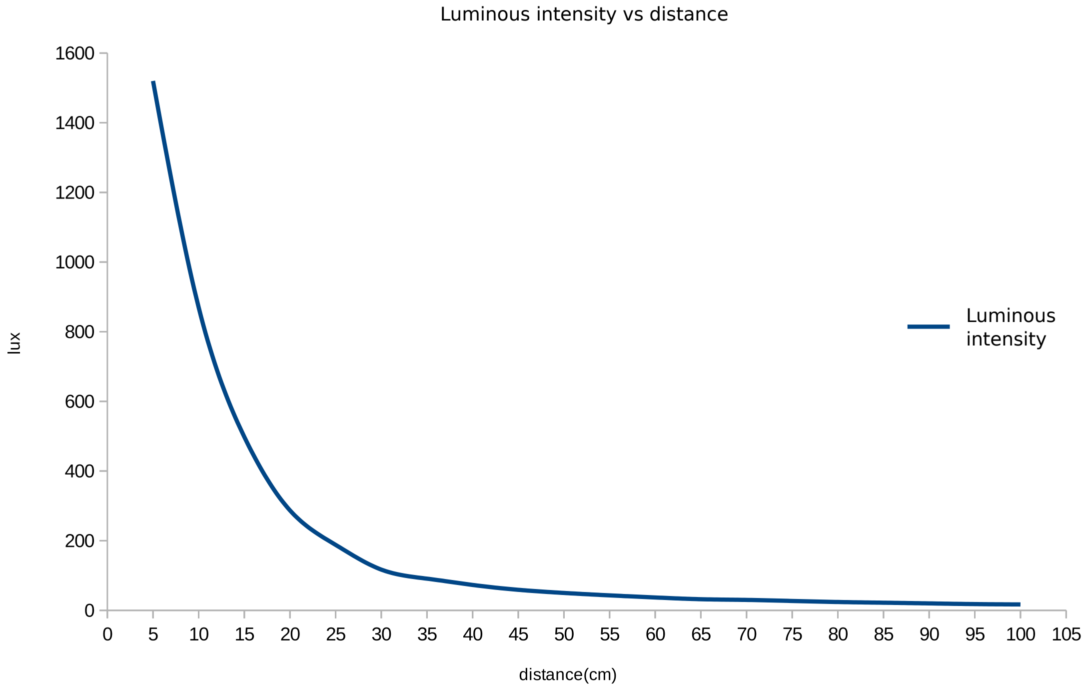

Figure 3.5: Attenuation of light with increasing distance

Consider the Figure 3.6, consisting of a light transmitter (Tx) and a receiver (Rx). The receiver is at a distance d from the transmitter. Light rays comingg from the Tx and received by the Rx create an angle ψ with the normal. This angle is known as the irradiation angle. The angle at which Rx receives these incident rays is knows as the incident angle and is denoted by θ. The angular distribution of the radiation intensity patterns is modelled using a generalized Lambertian radiant intensity with the following distribution [25]:

$$R_0(\psi) = \begin{cases} \frac{(m+1)}{2\pi}\cos^m(\psi) & \text{for} \quad \psi \in [-\pi/2, \pi/2], \\ 0 & \text{for} \quad \psi \geq \pi/2 \end{cases} \tag{3.2}$$

Using 3.2, a channel loss or attenuation model for this system can be described using the following equation:

$$H(0) = A_{eff} \cdot \frac{[m+1]}{2\pi d^2} \cdot \cos^m(\psi) \cdot \cos\theta \tag{3.3}$$

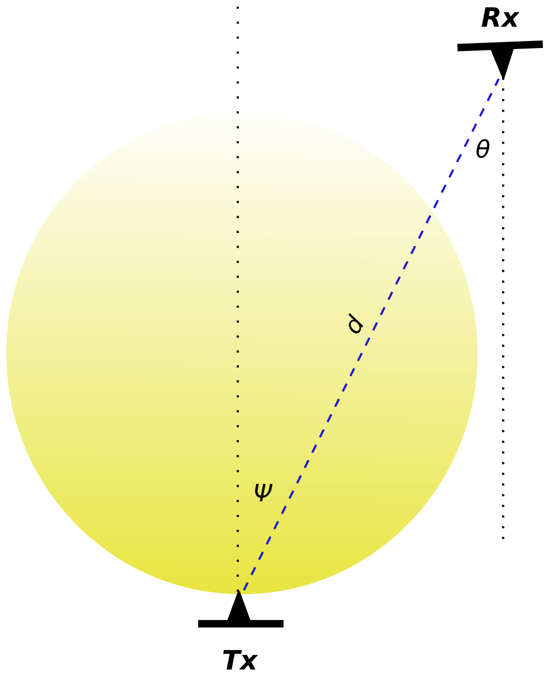

Figure 3.6: Channel loss in visible light

In this equation, $H(0)$ represents channel loss. There are some constants in this equation such as :

$\mathbf{A_{eff}}$: effective area of the receiver. If the receiver is a photodiode, then the effective area of the photodiode sensor.

m : Lambertian order of the receiver.

Apart from theses constants, the channel loss for visible light depends on the irradiation angle (ψ) of the transmitter, the incidence angle (θ) of the receiver, and the distance between them (d).

Received Power

Let us consider that the total optical power from the transmitter is denoted by P_t. Then we can describe the received power using the following equation:

$$P_r = P_t \cdot H(0) + N \tag{3.4}$$

where P_r is received power and N refers to noise. A simplified equation for ideal environments with out noise would then be:

$$P_r = P_t \cdot H(0) \tag{3.5}$$

By combining equations 3.3 and 3.5, the received power can be described as:

$$P_r = P_t \cdot A_{eff} \cdot \frac{[m+1]}{2\pi d^2} \cdot \cos^m(\psi) \cdot \cos(\theta) \tag{3.6}$$

Furthermore, we can group terms for effective area of photodiode, optical concentrator and other constants whose value won't change, to obtain a condensed form of the equation :

$$\begin{aligned} P_r &= T \cdot \frac{[m+1]}{d^2} \cdot \cos^m(\psi) \cdot \cos(\theta) \\ \text{where,} & \\ T &= \frac{P_t \cdot A_{eff}}{2\pi} \end{aligned} \tag{3.7}$$

3.3 Localization Method

In previous sections, we discussed how the intensity of light changes within a radiation pattern using Lambert's Cosine Law. We also described a mathematical order which defined the shape of radiation patterns. Lastly, a channel loss model for light was introduced combining both these things. In this section, we discuss the possible locations for a receiver and propose a localization method using the channel loss model.

Let us consider a scenario where a beacon (transmitter) transmits/radiates in every direction, and there exists a target (receiver) which must be localized. Such a scenario can be illustrated by Figure 3.7. Looking at this we can say that, based on the received signal strength, the receiver or target can be present on a circle around the transmitter. Now, because of this, rotating the beacon around its axis will introduce no change in the received signal strength as measured by the target, i.e. a change in the orientation will amount to no change in the received power at the target. In order to localize the target, we would need more beacons as each beacon would provide a new circle of points where the target might be present. The target can be eventually found at the intersection of these circles.

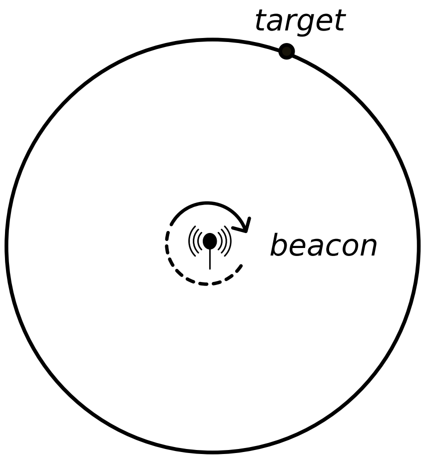

Figure 3.7: Scenario where transmission is omnidirectional.

In the case of light, things are a little different, because of some unique properties of light propagation patterns. Consider Figure 3.8, consisting of a light source and also a target to localize. In this case, if the light source is slightly rotated, it would also affect the radiation pattern. This rotation would introduce a change in the received power at the target, which can be measured. The possible locations of a target depend on the receive power, radiation pattern of the light source and other properties like incidence and irradiation angles. A change in the orientation of the beacon will cause a measurable change in the received power at the target, which corresponds to a new set of locations. In our proposed localization method, we can model these changes in received power and orientation to obtain the location of a target.

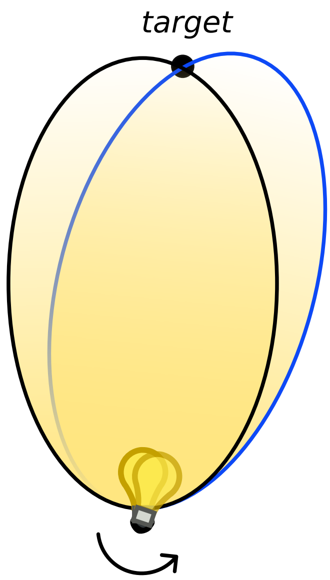

Figure 3.8: Change in orientation of transmitter, moves the radiation pattern.

3.3.1 Possible Positions for a Node

As we move a receiver away from the transmitter, the power measured at the receiver decreases. But in case of visible light, this loss of power also depends on the angle of emitted light as mentioned in equation 3.3. Consider the figure 3.9, comprising of a transmitter and a receiver at some orientations with respect to north. The receiver is placed at a distance from the transmitter, and measures some received power R. Now, if the receiver measures a power R at location **A**, then it is also possible for it to be closer to the transmitter at location **B** and receive the same amount of power R, provided it is at an angle.

Also, as the radiation patterns for light are symmetric, we can also infer that, the receiver can measure the same power R at location C. From this we can conclude that for a measured power R, a receiver can be present in multiple positions with respect to the transmitter.

Contours

The next step involves calculating all the possible positions for a receiver, but before that we must define one *state* in our system. Let us not forget, that the nodes in our system are mobile which means that both the transmitter and receiver can orient themselves in any direction. A state S can thus be defined as follows:

$$S = (t, r, R) \tag{3.8}$$

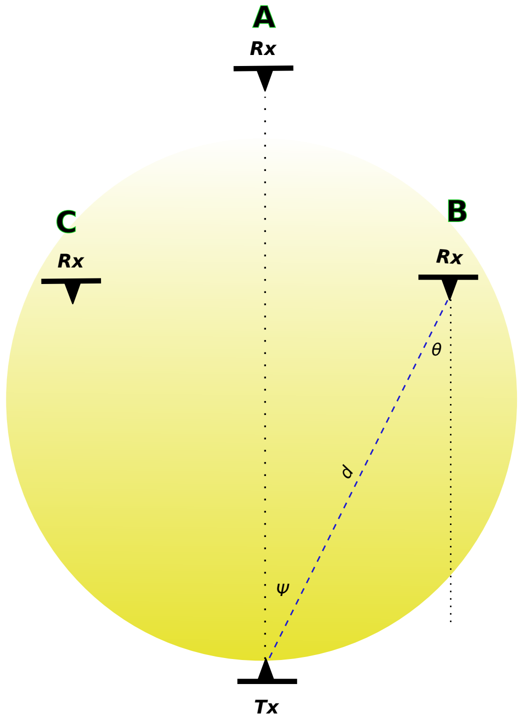

Figure 3.9: Multiple possible positions for a receiver node.

where,
t is orientation of the transmitter with respect to North,

r is orientation of the receiver with respect to North,

R is the received power.

To find all the possible positions for the receiver, we performed an experiment in which the received power was measured while moving the receiver in a horizontal 'scanning' motion with respect to the transmitter. This horizontal 'scan' was performed at different distances from the transmitter as illustrated in Figure 3.10. Each scan would provide two locations where received power was R. Collectively all such points at different distances from Tx, formed a *contour* of points for which the measured received power is the same.

From this we can infer that:

> *For a given state S of the system, a receiver can be in multiple positions, which together form a contour of points where the measured received power is the same.*

This also means, that for a given state S, this contour represents all the places a

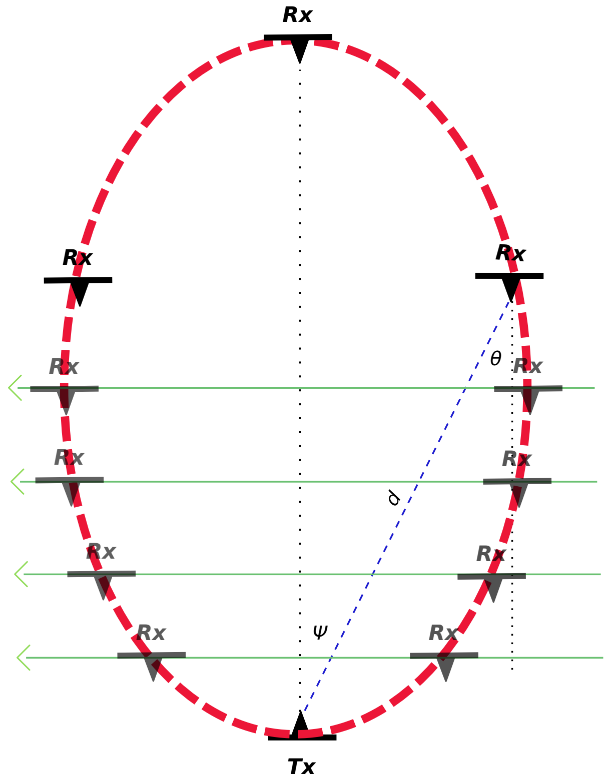

Figure 3.10: A Contour showing all the positions a receiver can be in a given state.

receiver can be.

3.3.2 Intersection of contours

Each contour corresponds to a specific state of the system. Or simply, the shape and size of a contour are directly related to the orientations of the transmitter and receiver. A change in the orientation of either of them would modify this contour. A system in a state S_1 would produce a contour as described in Figure 3.11a. A slight change in the orientation and only the orientation either of the transmitter or receiver would modify the shape of this contour. This state S_2 can be seen in Figure 3.11b. By looking at both these states, we believe that these two contours would intersect only at one point, and the receiver should be located at this intersection. This intersection of contours is shown in Figure 3.11c. It is important to note that, during this state change there is no change in positions of both TX and Rx.

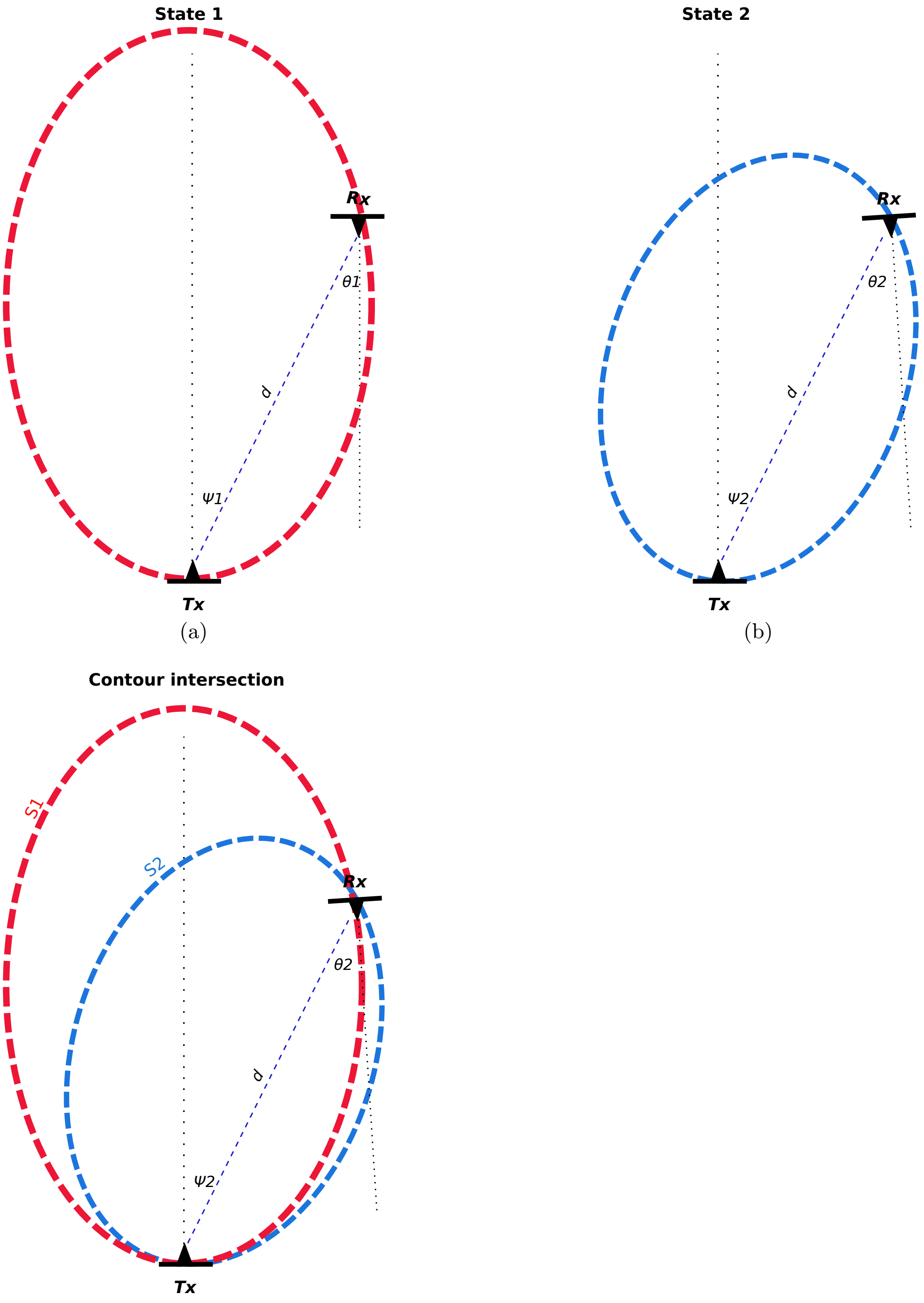

(a) (b) (c)

Figure 3.11: Localization using intersection of contours

3.3.3 Model Validation

The proposed hypothesis about intersection of contours can be proved mathematically as well as experimentally. To validate this mathematically, we can revisit the condensed equation 3.7 for received power.

Let us assume, that our system is in state S_1, where the orientations of the transmitter and receiver with respect to north are t_1, r_1, and the received power measured is R_1. Using equation 3.7, we can describe the received power for state S_1 as follows:

$$\text{For } S_1 = (t_1, r_1.R_1)$$
$$R_1 = T \cdot \frac{[m+1]}{d^2} \cdot \cos^m(\psi_1) \cdot \cos(\theta_1) \tag{3.9}$$

A similar equation can derived for state S_2, where the orientations of the transmitter and receiver are t_2 and r_2. Consequently, the received power for this state is R_2.

$$\text{For } S_2 = (t_2, r_2.R_2)$$
$$R_2 = T \cdot \frac{[m+1]}{d^2} \cdot \cos^m(\psi_2) \cdot \cos(\theta_2) \tag{3.10}$$

Looking at equations 3.9 and 3.10 we can infer that, they cannot be solved in their present form because, for two equations, we have a total of five unknown variables. These unknowns are namely ψ_1, ψ_2, the irradiation angles for the two states, θ_1, θ_2, incidence angles and d, the distance between the transmitter and receiver. However, after much analysis and experimentation, some dependencies were found between these unknowns.

The incidence angle θ is a function of the orientations of the transmitter and receiver as well as the irradiation angle ψ.This dependency can be applied for the incidence angles θ_1, θ_2 in both the states.

Dependency 1: $\theta_1 = f(t_1, r_1, \psi_1)$

Dependency 2: $\theta_2 = f(t_2, r_2, \psi_2)$

This relation between the incidence angle and irradiation angle can be illustrated by the Figure 3.12.

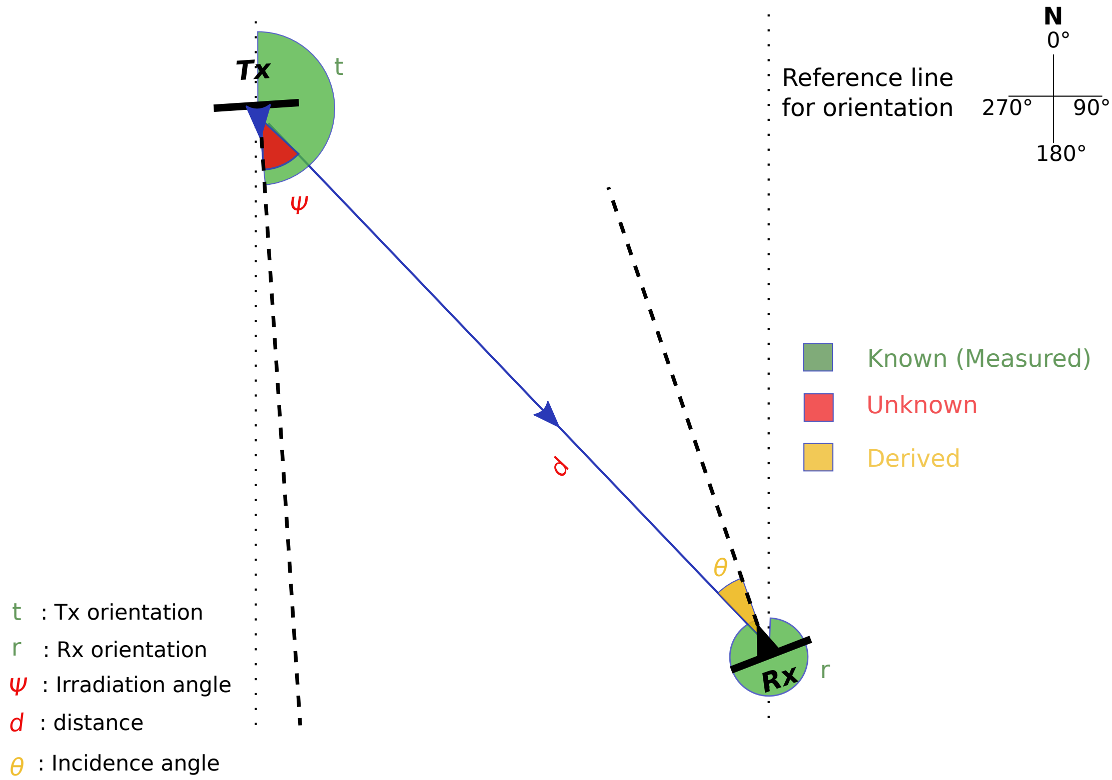

Figure 3.12: Relation between incidence angle and irradiation angle.

From this figure, the following derivations can be made:
Let the relative angle between nodes be *rel*.

$$rel = r - t$$

then θ can be described as:

$$\theta = \pi + \psi - rel$$

Moreover, the irradiation angle ψ_2 for state S_2, itself is a function of the irradiation angle ψ_1 and the orientations of the transmitter in both the states.

Dependency 3: $\psi_2 = f(t_1, t_2, \psi_1)$

This dependency is illustrated in Figure 3.13. The difference in the orientations of the transmitters for states S_1 and S_2 can be described as:

$$\Delta t = t_1 - t_2$$

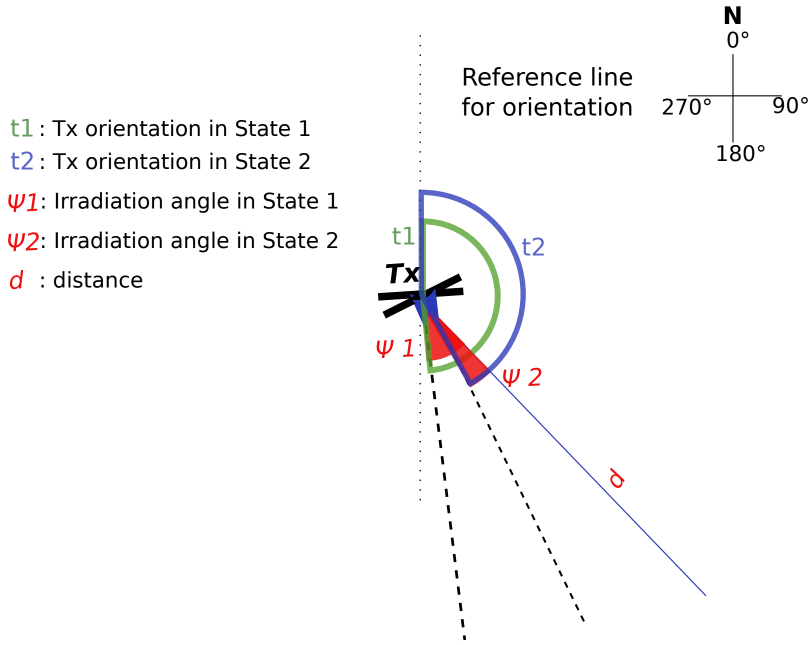

Figure 3.13: Relation between irradiation angles of two states.

Using this we can derive:

$$\psi_2 = \Delta t + \psi_1$$

Taking into account the above mentioned dependencies, the equations 3.9 and 3.10 can be re-written as:

$$\begin{aligned} S_1 \rightarrow R_1 &= T \cdot \frac{[m+1]}{d^2} \cdot \cos^m(\psi_1) \cdot \cos(f(t_1, r_1, \psi_1)) \\ S_2 \rightarrow R_2 &= T \cdot \frac{[m+1]}{d^2} \cdot \cos^m(f(t_1, t_2, \psi_1)) \cdot \cos(f(t_1, t_2, r_1, r_2, \psi_1)) \end{aligned} \tag{3.11}$$

This is now a system of two equations with two unknowns which can be solved to give a solution. But, as this system of equations is quite complex, a closed form expression has not yet been formulated. However, this model was also validated with the help of experiments, which do indeed prove that a unique solution can be obtained. The experimental results and analysis will be discussed in the upcoming chapter.

Chapter 4

Implementation

In the previous chapter we discussed the properties of radiation patterns of light and how they can be used to localize an object in mobile settings. This chapter describes the hardware and software platform used for implementing the proposed localization algorithm. The proposed method also involves communication between the nodes using visible light. We go through the details and requirements for having localization as a part of the visible light communication protocol.

4.1 Hardware and Software setup

The hardware and software setup includes the actual platform on which the experiments were conducted as well as the software framework used for localization.

4.1.1 OpenVLC

OpenVLC is an open source project, which provides a flexible, low-cost visible light communication platform. It is a general purpose software-defined VLC platform, which can be used for fast prototyping of LiFi networks [19]. OpenVLC is an extension or a cape for the BeagleBone Black embedded platform [1].

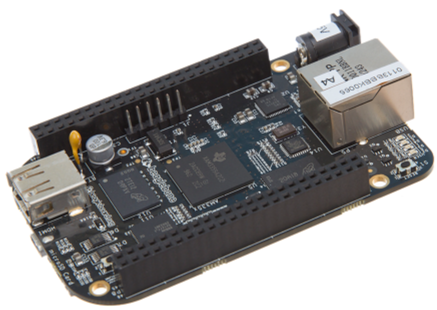

Figure 4.1: The Beaglebone Black embedded platform.

The BeagleBone black as shown in Figure 4.1 is a small credit-card sized low power embedded system comprising of an ARM Cortex A8 processor. The operating system for this platform is a linux distribution, Debian modified to support OpenVLC requirements. This embedded platform includes 46 pin-headers, which can be used to connect multiple devices. Many extensions or capes can be added to the system through these pin-headers. OpenVLC is an example of such extensions [2].

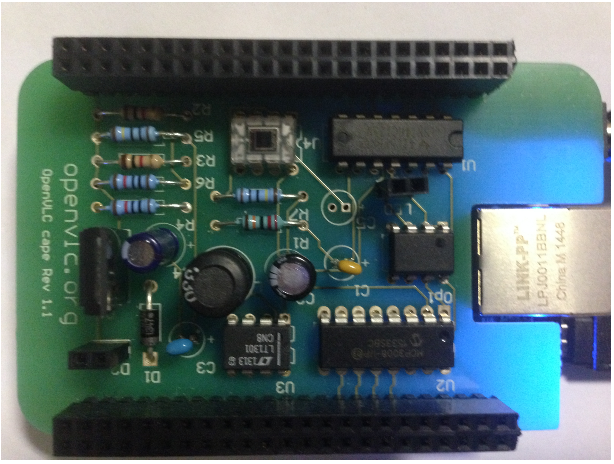

Figure 4.2: OpenVLC cape attached to a BeagleBone Black [2].

Figure 4.2, shows an OpenVLC cape attached to a BeagleBone Black. The cape is a VLC transceiver, and consists of three optical components. These include a High-Power LED, a low power LED, and a photodiode. The photodiode used is OPT101, as shown in figure 4.3, and acts as the primary receiver.

Figure 4.3: Receiver photodiodde OPT101.

The two LEds used can be seen in the Figure 4.4. The low power LED is a standard 13mm red CREE LED. This LED can be used both as a transmitter and a receiver by switching it from forward bias to reverse bias mode. The high power LED is actually of a combination of 6 SMD5050 LEDs in a cluster. It must be noted that, high power in this case refers to a 1 watt power consumption by the LED cluster, which is very low compared to the 10 - 20W LED lamps used in rooms.

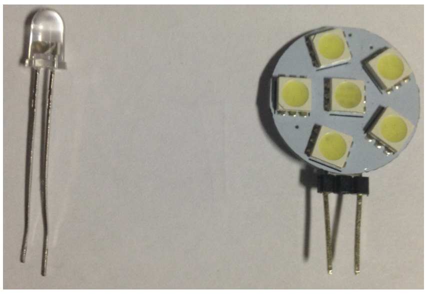

Figure 4.4: A low power and a high power LED

A high level overview about how all these components are connected and can be used for communication is illustrated in Figure 4.5.

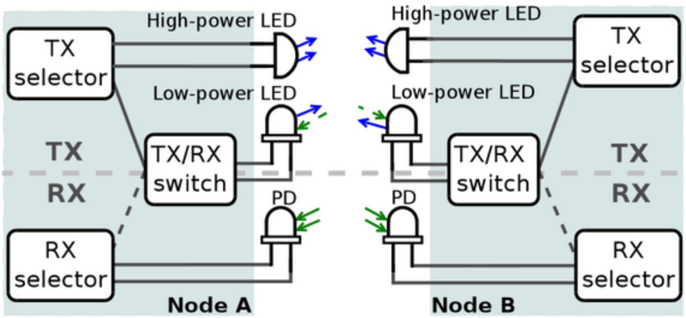

Figure 4.5: Overview of components connected in OpenVLC.

On the software side, communication is handled using an OpenVLC *network driver*. For localization, raw data from the photodiode through an ADC(Analog to Digital Converter) was retrieved from the kernel space with the help of kernel modules. For localization to be a part of the communication protocol, this information must be incorporated in the VLC MAC/Data link layer. This layer, along with others is shown in Figure 4.6.

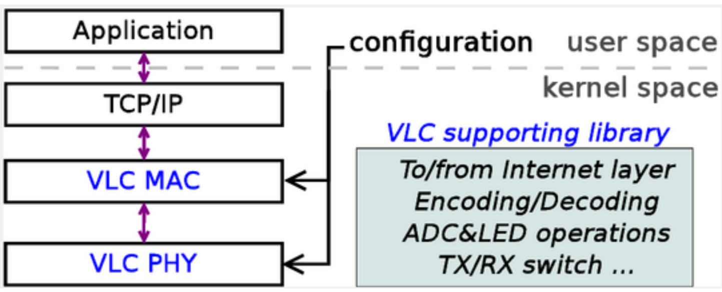

Figure 4.6: Visible light communication layers.

4.1.2 Orientation sensors

The orientation of a node plays a crucial part in the localization algorithm. The node in our system have a single reference which is their orientation with respect to magnetic north. This information can be obtained with the help of specific sensors, most of which are already present in smart-phones now-a-days. At first an Android smart-phone was used to provide this orientation information. The smart-phone used sensors like magnetometer and accelerometer to retrieve a nodes orientation, which were sent to a BeagleBone using a USB cable. The sampling rate of the phone was around 500Hz and the data was sent through a USB cable.

An alternative to using a smartphone as an orientation sensor was the *sensor fusion* board BNO055. This sensor board comprised of multiple sensors such as the accelerometer, gyroscope and magnetometer which had a higher sampling rate. This sensor was more robust to noise and other disturbances, as it could combine the data from all the sensors on board to calculate the orientation. Figure 4.7a shows the BeagleBone board connected with an Android smartphone.

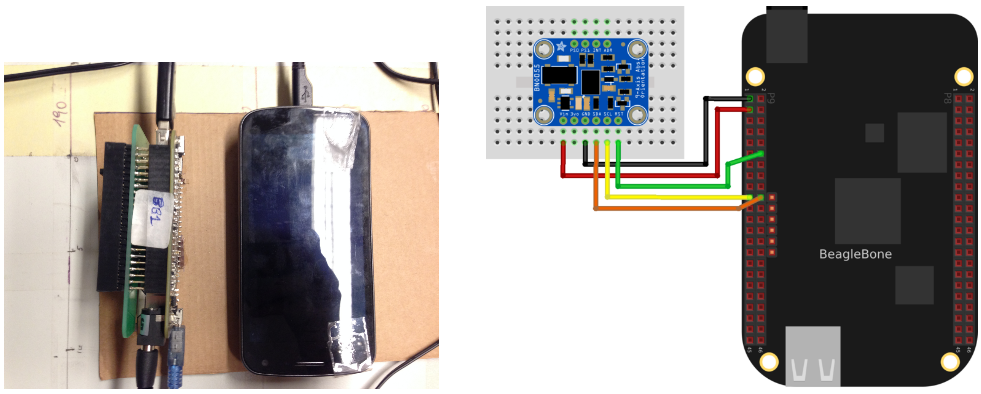

(a) Android Smartphone connected with a Beaglebone via USB cable.

(b) BNO055 sensor board connected with a Beaglebone via SPI interface [3].

Figure 4.7: Using a smartphone and a dedicated sensor for orientation information with the BeagleBone.

4.1.3 Software Implementation

Orientation information from the Android smartphone was retrieved using an Android application. When attached to the BeagleBone, both the smartphone and the board were assigned a local IP address. The orientation data was then sent to the BeagleBone through the network via a USB cable using the User Datagram Protocol (UDP). The sensor BNO055 was attached to the BeagleBone using the Serial Peripheral Interface (SPI.) Data from this sensor was retrieved with the help of Adafruit library which is available online [3].

An overview of how all these components were connected and their interactions can be illustrated by Figure 4.8. Interaction with the OpenVLC cape was done using a kernel module/driver. The current driver for OpenVLC provides a network interface which can be used to send UDP or TCP/IP packets. We modify this driver, to obtain raw values from the photodiode, which are required for localization. Data from the kernel module is sent to the localization program using the *proc file system*. The *proc file system* provides a simple file I/O interface which can be used to share data between kernel and user space. A listener program obtains information from the orientation sensors by continuously polling a UDP port. This listener thread runs parallel to the main localization program, which combines data from this port and the data shared through the *proc file system* to calculate the position.

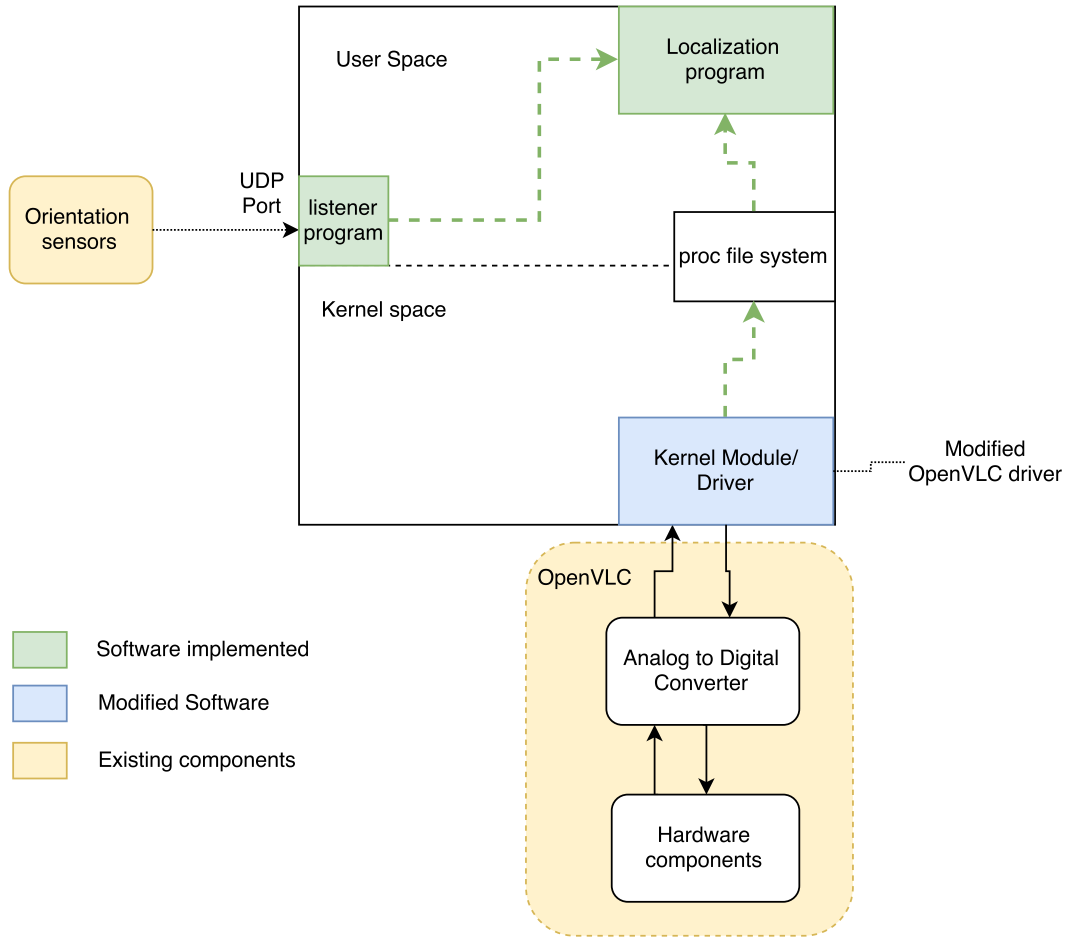

Figure 4.8: Overview of hardware and software interaction

The positions calculated were further visualized using a real-time graph with the help of the *matplotlib* library and Python. Figure 4.9 shows how the localization was visualized.

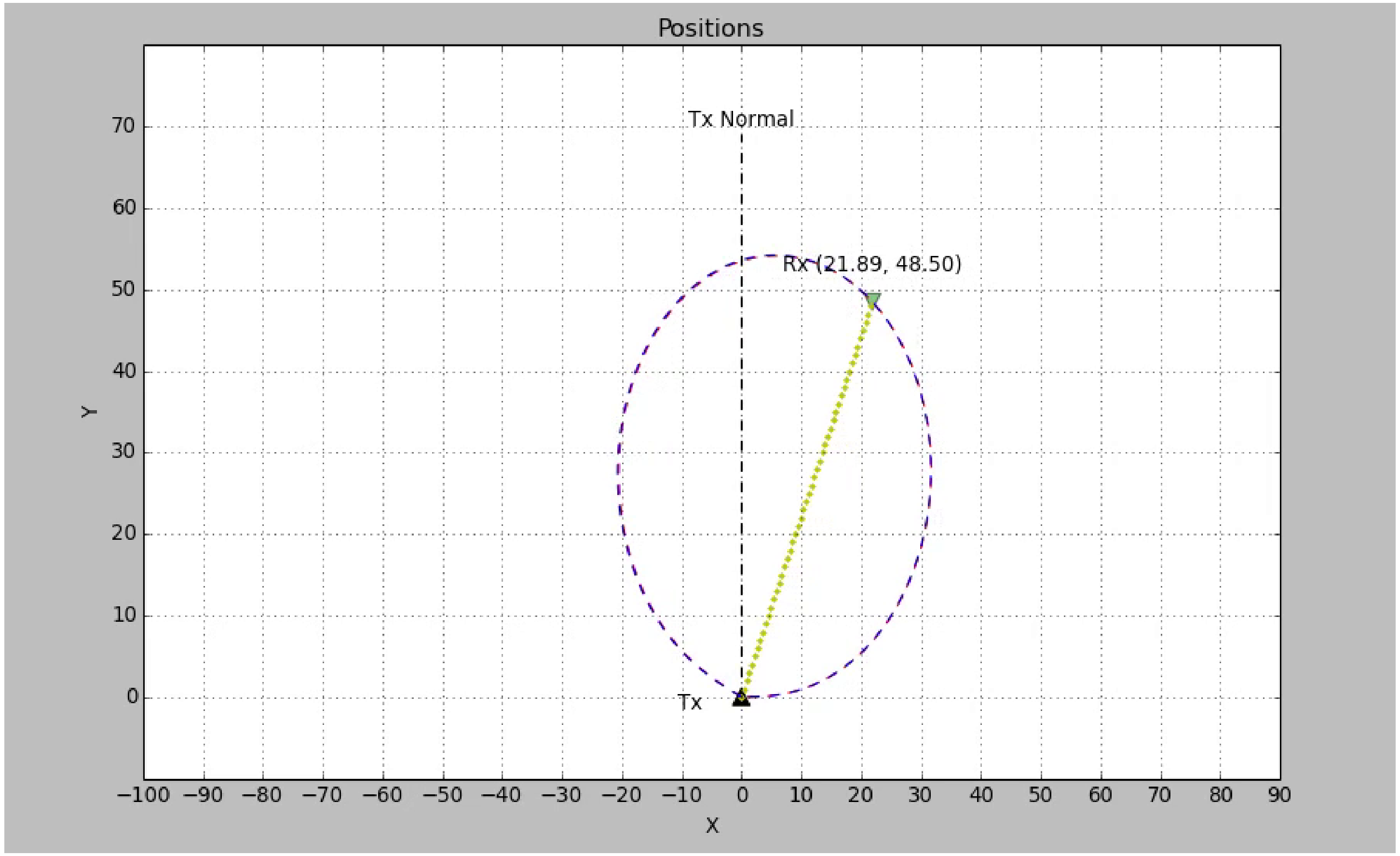

Figure 4.9: Using matplotlib and Python to visualize localization

4.2 Localization as a part of communication

Communication using visible light is vital for the proposed localization method. In order to calculate the position of a receiver relative to the transmitter, important information like the optical characteristics and orientation of the transmitter must be relayed. To find the position of a receiver, we primarily need to measure the received power and the orientations of both Tx and Rx. But, some other constants, such as the total output power and lambertian order of the transmitter also need to be shared. This is done using VLC. In our system, visible light communication is done using the OpenVLC cape. OpenVLC uses OOK modulation and the frame format used in transmission is shown in Figure 4.10. For the purpose of this project, data relevant for localization, such as the received power and optical constants, was obtained through different sections of this frame format. By modifying the OpenVLC network driver, the preamble of a single data frame in the MAC layer was used to determine the received power. The optical properties of the transmitter and its orientation were transmitted as the payload.

Frame Format for VLC data link layer (MAC)

FIELD	Preamble	SFD	Length	Destination	Source	Protocol	Payload	CRC
BYTE	3	1	2	2	2	2	0...1500	2

Figure 4.10: OpenVLC Frame format in the MAC layer.

4.2.1 Measuring received power

The preamble of the frame format is 3 Bytes long which means that it comprises of 24 bits. These 24 bits of the preamble are also used for synchronization, so that the rest of the frame can be easily decoded. For synchronization the preamble contains data = 0xaa, which when converted to binary looks like 01010...similar to a clock signal.

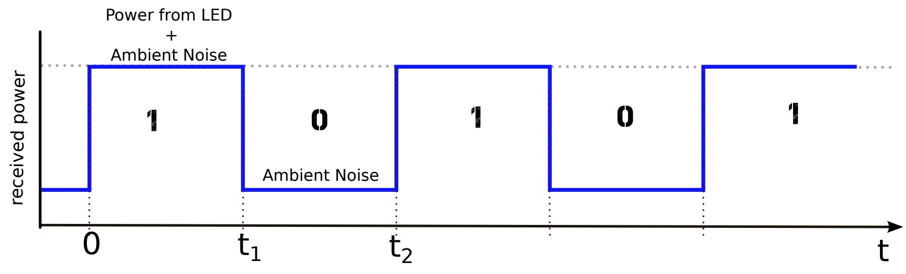

Figure 4.11: Measured power during preamble transmission.

From this preamble, information pertaining to power received from an LED source can be extracted. Every high symbol of the preamble, corresponds to the ON state of the LED transmitter. Thus, a measurement for every high symbol comprises of power received from the LED transmitter, as well as ambient noise. Similarly, every low symbol of the preamble corresponds to an off state of the LED transmitter, The only power measured during this state is the power received from ambient light. So, for one data frame, the received power from a transmitter can be calculated by subtracting these two measurements made during the high and low symbols of the preamble. Figure 4.11 shows the power measured while reading the preamble.

This method proved to be accurate, however continuous testing highlighted an anomaly. The preamble is made up of high and low symbols, which in fact are values from the photodiode. It was observed that, after a certain duration, for a few data frames, the values in their preamble were skewed. These values didn't correspond with the ambient noise levels and the power received from the light source, and thus couldn't be used for localization. Consequently, there was a need to separate these *bad* preambles from the good ones. Investigation of the OpenVLC driver helped us understand the cause of this anomaly. In communication, in order to receive data, symbols used for transmission must be identified or sampled. In case of OpenVLC, these symbols are the on and off states of a light source, where each state has a fixed duration. This duration is decided by the frequency at which data is modulated, and can be configured through the OpenVLC network driver configuration.

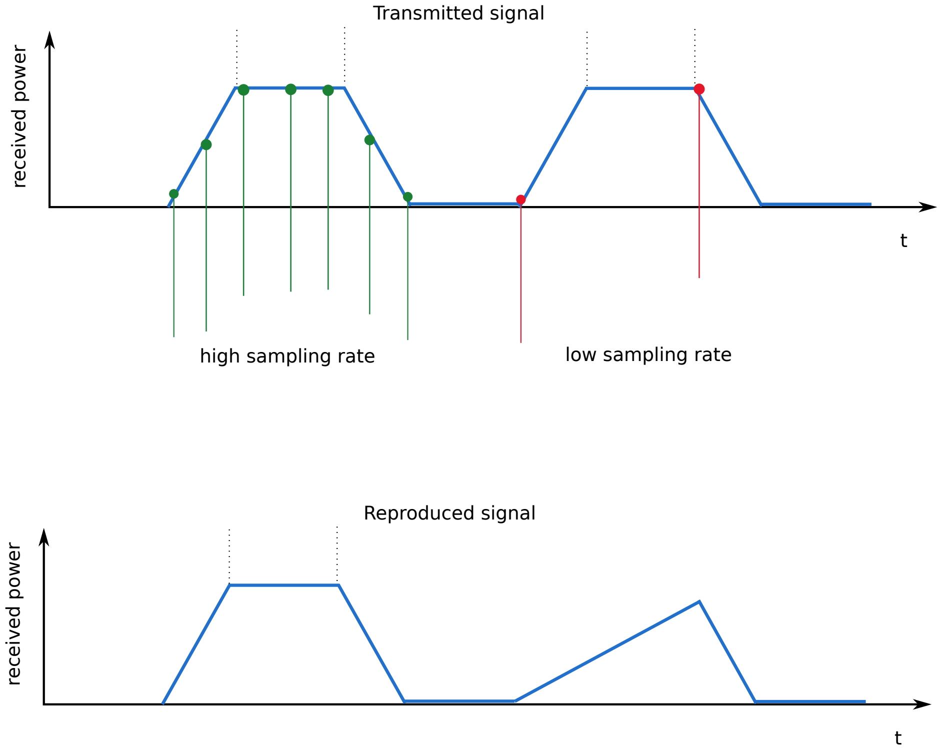

Figure 4.12: Effect of sampling rate on signal representation.

To identify these states or symbols, ideally they must be sampled multiple times within the duration of each symbol. A high sampling rate ensures a better representation of the symbol. However, in case of OpenVLC, only a single measurement was used to identify a symbol. A low sampling rate such as this introduces anomalies in representing the symbols. This can be illustrated by Figure 4.12. We experimented with different methods to deal with the anomalous preambles. One of them was based on calculating the standard deviation of either the high or low symbols. If the deviation was larger than a certain threshold, then the preamble was skewed and thus discarded. Also, in our implementation we chose the highest and the lowest symbols of the preamble to get a better representation. However, a much easier solution was found in reducing the frequency of data modulation. This increased the duration for each symbol because of which the probability of getting an anomalous symbol was greatly reduced.

Chapter 5

Results and Evaluation

In this chapter, we analyse the optical characteristics of different types of transmitters and receivers which can be used in our system. Aspects of the model proposed in Chapter 3 are also validated and visualized with the help of Matlab simulations. Lastly we take a look at the test environment and evaluate the results for two scenarios in which localization can be performed.

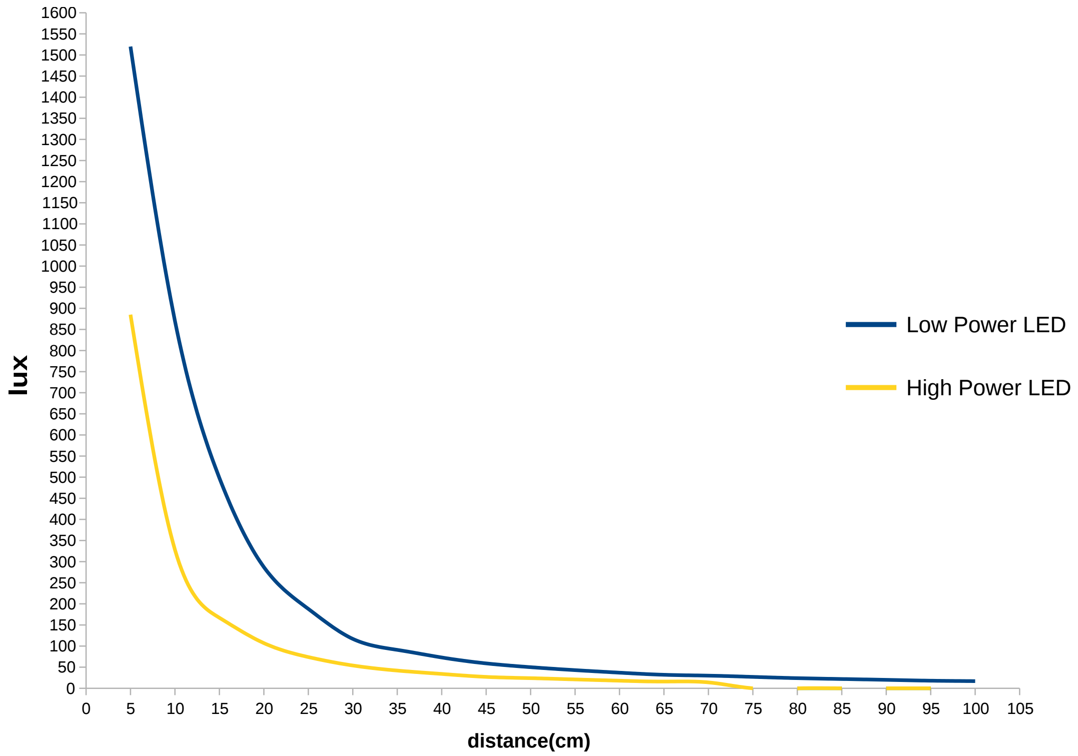

Figure 5.1: Channel loss observed for different light sources when both the receiver and transmitter are aligned.

In Chapter 4, the Figure 4.4 described the two different types of light sources or transmitters used for experiments. Both light sources, a high power and a low power LED have different optical characteristics. The high power LED has a very broad field of view with a short range of illumination, whereas the low power LED is very directional but with a long range. Consequently, the attenuation or channel loss for them are quite different. This can be seen in Figure 5.1.

Usually, one can expect to find the optical properties of a light source in the data sheet provided by its manufacturer. However, there are cases when such a document is unavailable, or a transmitter was constructed by combining multiple LEDs, like the High Power LED used in our experiments. In such instances, characteristics of a light source such as the *Lambertian Order(m)* can still be calculated.

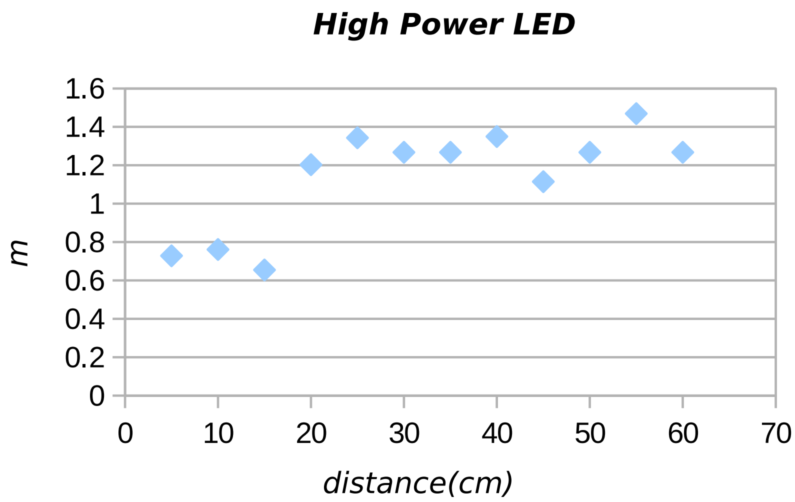

(a)

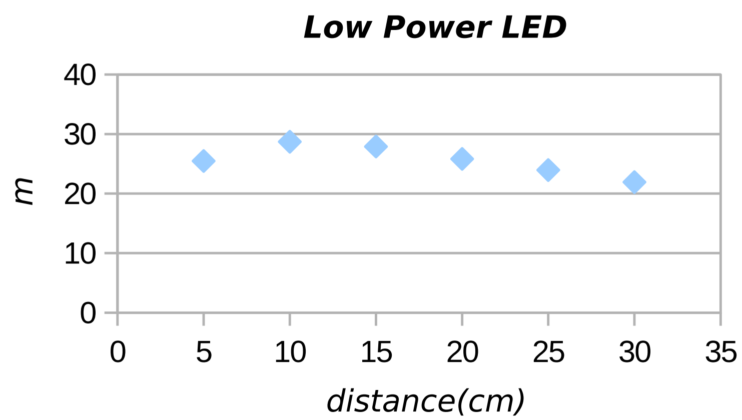

(b)

Figure 5.2: Experimental calculation of Lambertian order

This can be done with the help of the mathematical model for channel loss. During our experiments, for each of the light sources, measurements for received power were made at different distances and angles. These values were used in the equation 3.7, to reverse calculate the value m. Figure 5.2 depicts the calculated values of m for both the transmitters, at different distances. From this figure we can see, that the value of m for a high power LED is quite low, approximately around 1.2. This is apt, because the high power LED has a wide field of view and thus forms a broad radiation pattern which is supported by the low value of m. Similarly, the lambertian order for a low power LED was calculated at different distances. Unlike the high power LED, the value of m was observed to be quite high at around 25. A high value of m indicates a narrow radiation pattern, which is true in this case as the low power LED is a very directional source of light. Upcoming results and analysis were obtained by using the high power LED as a transmitter, as light from it was observed to spread across a much larger area. This provided us with a nice distribution of intensities which can be used for localization.

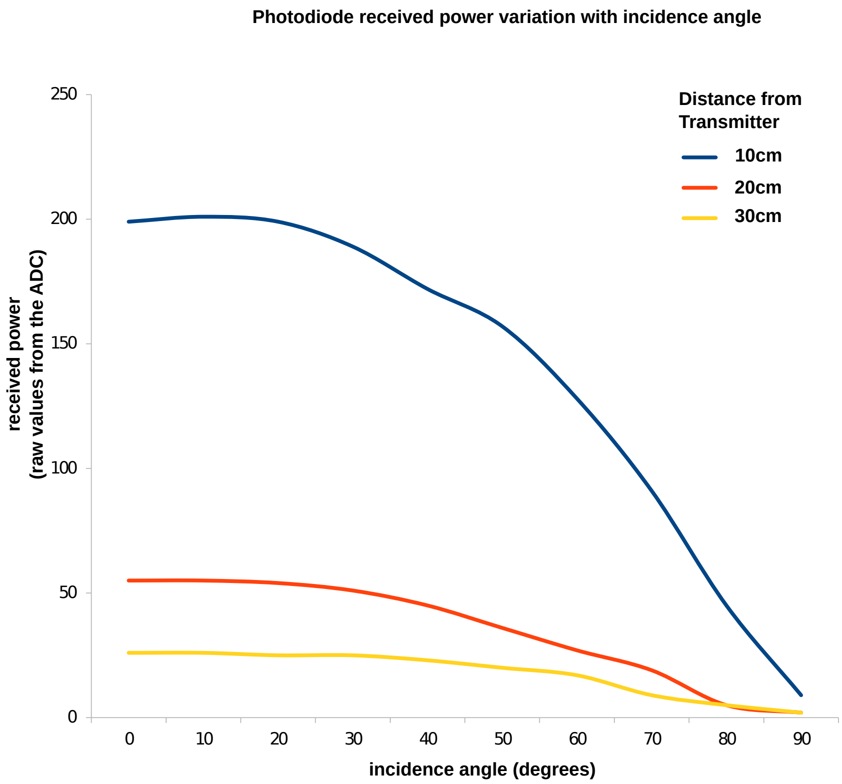

Figure 5.3: Response of photodiode with varying incident angles

Experiments were also conducted to analyse a photodiode as well as an LED as receivers. The low power LED when connected in reverse bias mode, acted as a receiver. However, the design of an LED, consists of a lens cap to boost transmission. This lens cap hinders the capability of using an LED as an effective receiver, because it reduces the field of view considerably. The photodiode on the other hand showed promising results, as it has a very wide field of view reaching almost 180°. Consequently, the photodiode had a better angular response and showed good resilience towards increasing distance.

Contour simulations

Figure 5.4 shows the changing shape of contours when the transmitter is at 0°, and the receiver orientation changes from 180° to 120°. With the help of the channel loss model in equation 3.3, the behaviour of these contours can be simulated.

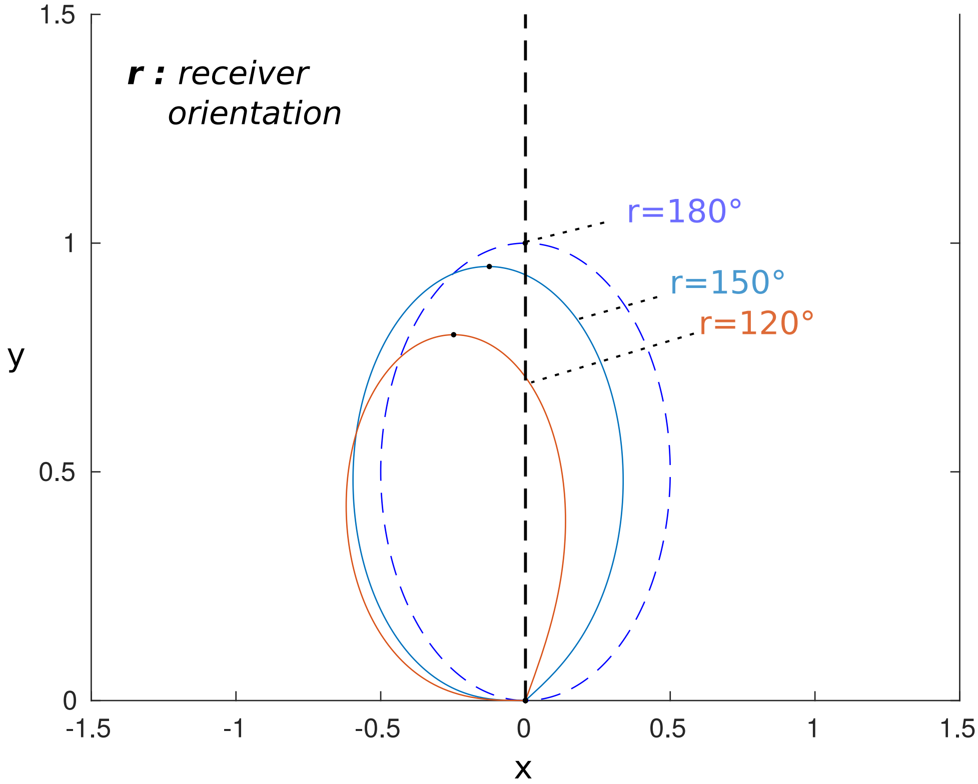

Figure 5.4: Changing contour shapes with varying receiver orientation

In section 3.3.1, we proposed that for a given state, a node or a receiver can be present at set of points, forming a contour. Experimental results as shown in Figure 5.5 validate this hypothesis by showing that after scanning the receiver in front of a transmitter, the same received power can be measured at different positions.

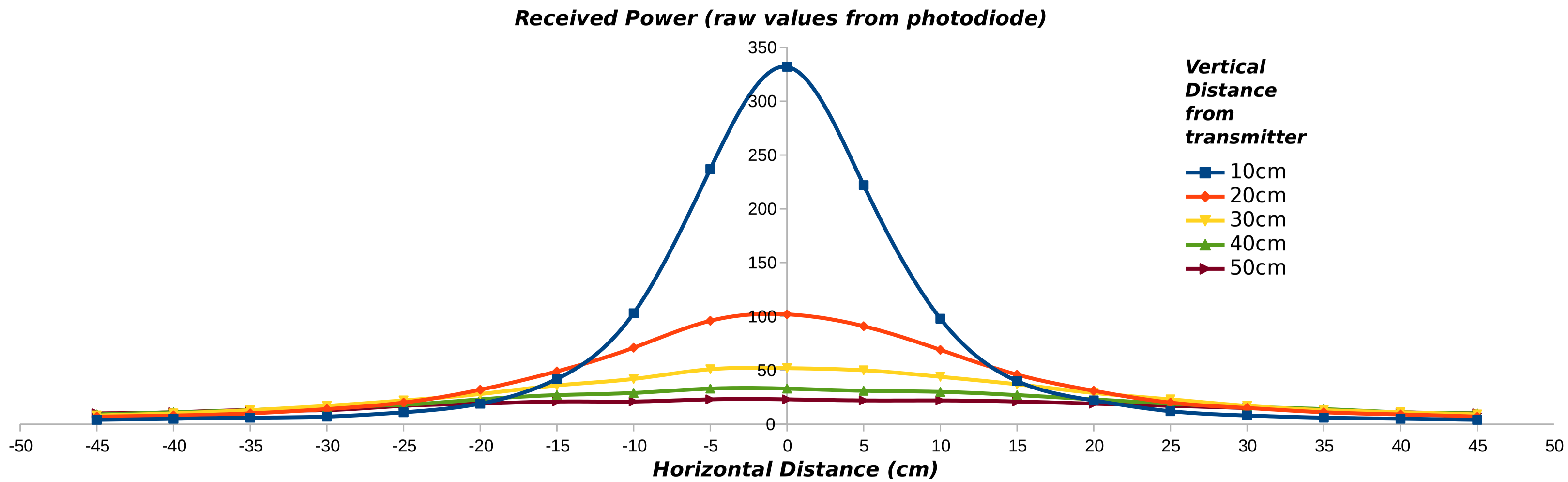

Figure 5.5: Measured received power after scanning for increasing distances

5.1 Test environment

Experiments were conducted in a controlled lighting environment. Initial results for model validation and analysis were conducted in near dark lighting conditions with an illumination level of approximately 3 lux. These results served as a benchmark for the remaining experiments. Further results, were conducted in normal office lighting conditions with illumination levels being around 200 lux. The high power led was chosen as a transmitter for all localization experiments because of its broad field of view. Also, the photodiode OPT101 was the receiver for all tests because it was much more reliable and efficient than using an LED as a receiver.

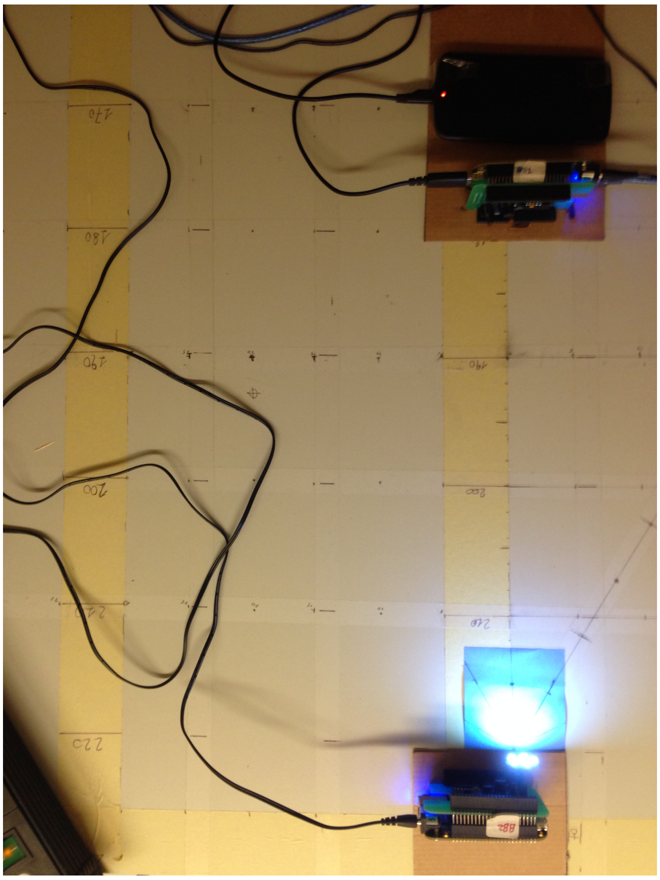

Figure 5.6: Test bench for measuring localization accuracy

Localization accuracy was measured using the setup shown in Figure 5.6. The test setup was a grid spanning $150cm \times 100cm$, with each cell of the grid having dimensions $10cm \times 10cm$.

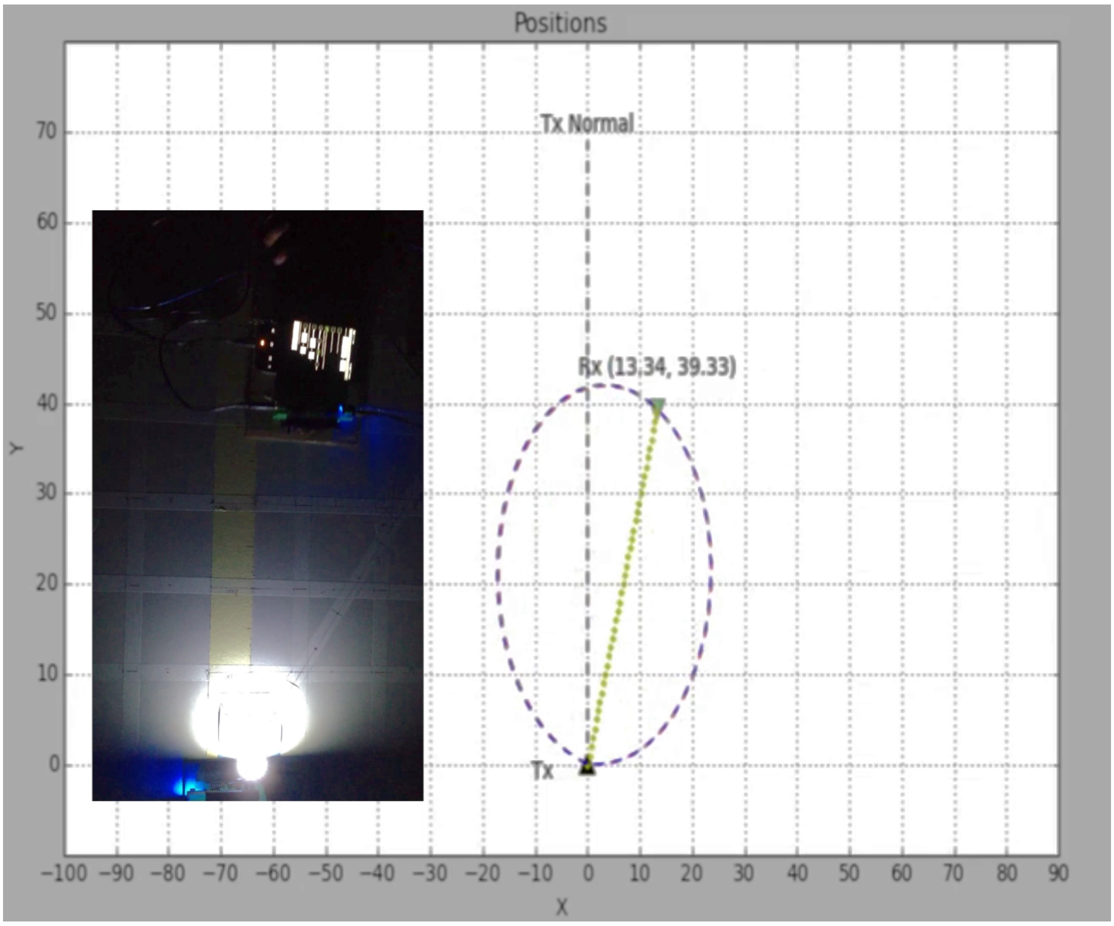

Figure 5.7: Experimental validation of localization model using real time location plotting.

5.2 Localization scenarios

The localization method was tested for two scenarios, a static case where only one node is mobile and a dynamic case where both nodes are mobile. The analysis involves a discussion on the accuracy and factors which affect them.

5.2.1 Static case

In the static case for localization, the position of one node was fixed. Initially this node behaved as a light source (Tx) and the other node which was mobile behaved as a receiver (Rx). Figures 5.6 and 5.8 illustrate this setup.

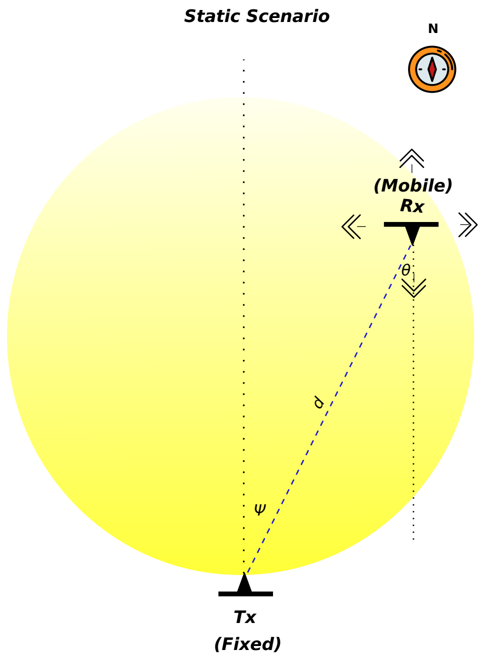

Figure 5.8: Test setup for static scenario

The location of a node was derived by solving the system of equations 3.11 described in Chapter 3. Using these equations, the two unknowns ψ (irradiation angle) and d (distance) from the node can be calculated. This was done first, in dark conditions without modulating the light from the transmitter. In this case, properties of the transmitter such as its orientation, total output power, and lambertian order were 'hard-coded' in the receiver. The results for these experiments serve as a benchmark for further experiments where the light signal was modulated to send data, and the positions were calculated in both dark and illuminated environments.

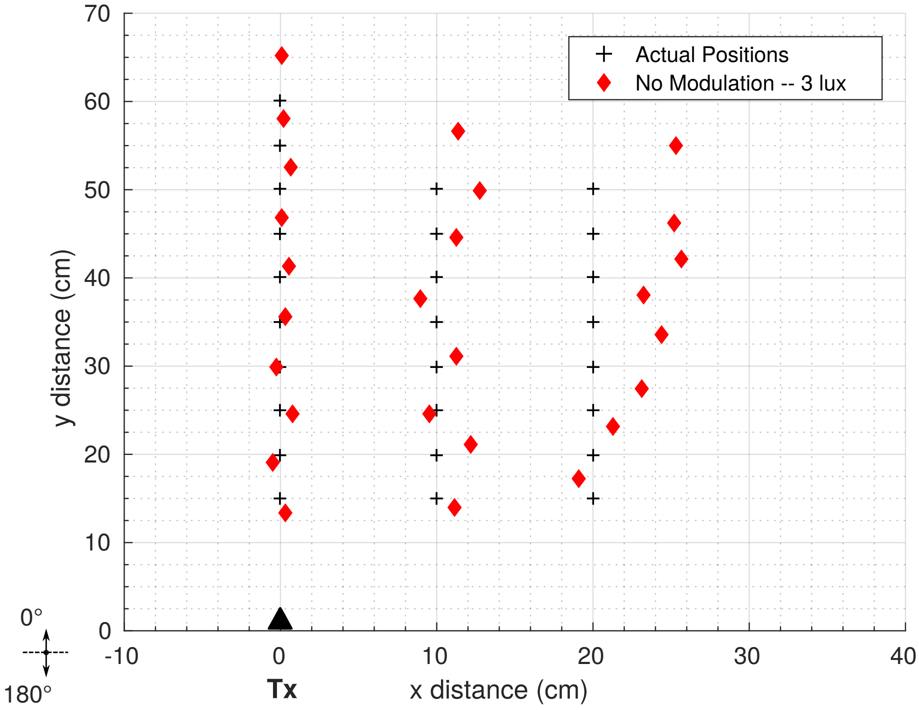

Figure 5.9: Positions measured for receiver without modulating light

Figure 5.9, shows the transmitter is static at position $(0, 0)$ with an orientation of $0°$. The transmitter in this case is just a source of light with no modulation. The receiver position was calculated at different distances from the transmitter in a dark environment with a noise level of 3 lux. Corresponding errors, in the x and y coordinates of these positions can be seen in figures 5.11 and 5.10. These graphs highlight an important trend, where the error in the positions of the receiver increase as we go further away from the transmitter.

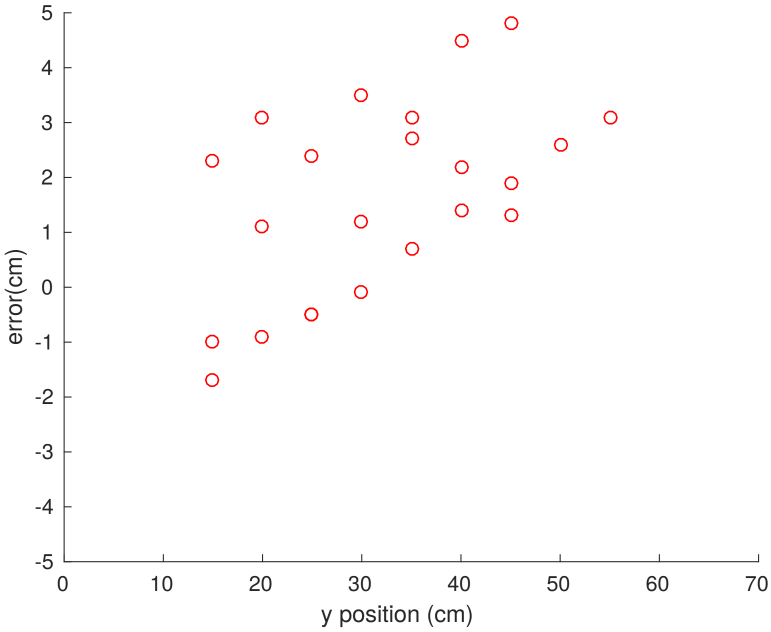

Figure 5.10: Y position errors while calculating receiver position in static case

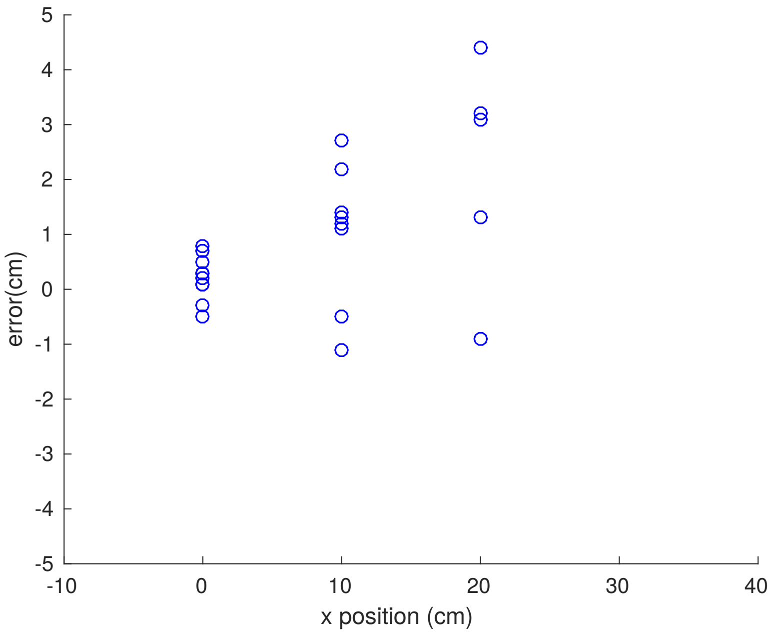

Figure 5.11: X position errors while calculating receiver position in static case

Analysis

During experiments, it was observed, that localization was difficult if the node was closer than 15cm. This is because at this distance the photodiode would saturate. As we move further away from the transmitter, we can see how the error trend in the x and y positions of the receiver from figures 5.11 and 5.10. Consider the localization results from figure 5.9, where the receiver was aligned with the transmitter i.e., $x = 0$ for the receiver and only the y distance was varied. A high accuracy for localization was observed between 20cm to 50cm (y-distance) from the transmitter, after which the error rate increases as we go further from the transmitter. The reason for the error to increase is because, after a certain distance, the photodiode used in our experiments is not sensitive enough .i.e., the values obtained from the photodiode didn't have enough granularity to pick up the subtle decrease of luminous intensity. This phenomenon can also be illustrated by Figure 5.12.

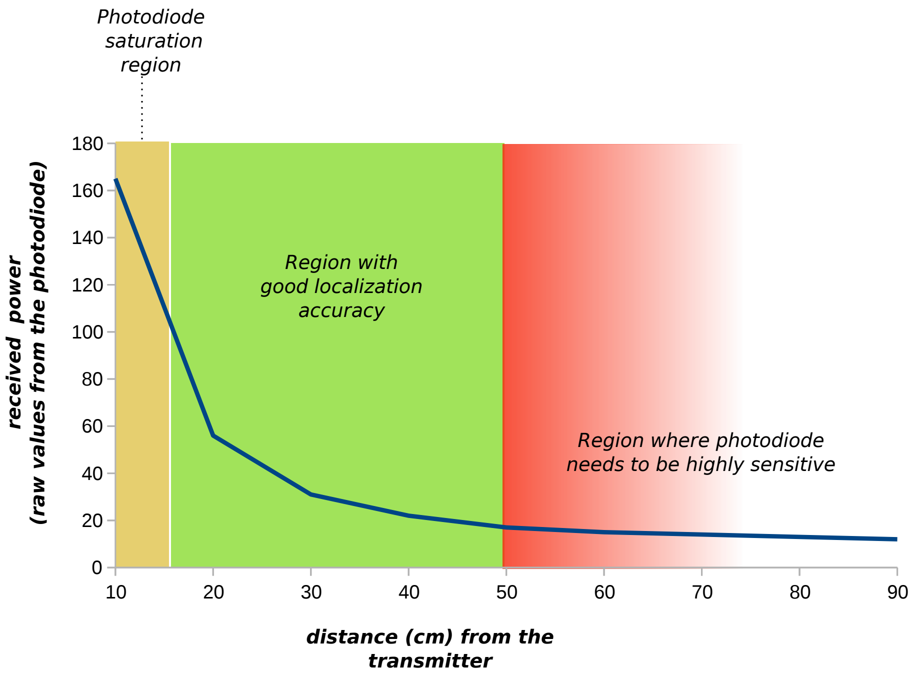

Figure 5.12: Regions with varying error rate for localization.

Moreover, we observe that error in localization increases significantly, as we move away from the transmitter along the x axis. This can be attributed to two reasons, with the limited sensitivity of the photodiode being one of them. The other reason for these errors can be explained using equation for received power in 3.7. From this equation we can see that received power is directly proportional to the cosine of the irradiation angle. As we move away from the transmitter in the x direction, this irradiation angle also increases. Subsequently, any errors in calculating this angle, which are mainly due to errors in the orientation sensor, have a large impact on the position of the receiver. Thus, limited sensitivity of the photodiode and errors in irradiation angle due to the orientation sensor, together contribute to errors in the position of a receiver.

Communication while Localization

The localization results from the previous section were obtained when the light from the transmitter was constantly on i.e., there was no modulation or communication using visible light, and the experiments were performed in a dark environment, with negligible ambient noise at around 3 lux. This was acceptable for experiments and validation of the model, however, this is not feasible for real world scenarios. We use these results, as a benchmark for experiments where the light signal was modulated in both dark and illuminated environments. Enabling VLC while localization required some modification of the existing OpenVLC network driver. Information relevant to localization such as orientation, output power and lambertian order of the transmitter, which were hard-coded earlier, are now embedded and extracted from the data frames sent by the light source.

Power received from a light source is calculated from the preamble of each of these data frames. As explained in section 4.2, this is done by measuring power during the transmission of high and low symbols of the preamble respectively, and then subtracting them to obtain the power received just from the light source. This way, *during the transmission of each data frame*, ambient noise can be measured and separated from the power measured by the photodiode. Subsequently, we can now also measure the power received from a light source under high ambient noise levels. The estimations of received power when the light signal was modulated, are compared with our benchmark results. These benchmark results are the received power measurements using a non-modulated light source in ideal dark lighting conditions. These measurements were obtained when both the Tx and Rx were aligned, and the receiver was placed at increasing distances from the transmitter.

Analysis

Figure 5.13 shows the error in received power from a modulating light source when compared to a non-modulating light source in dark conditions (3 lux). The error in the received power measurements was observed to be quite low. Measurements were also done in high ambient noise conditions of 200 lux, which gave similar results. The reason for this is that, while modulating the light signal, we are also constantly recording the power measured from ambient noise. Using the general equation of power received in eq. 3.4, we can easily separate the power received from the light source and ambient noise. Changes in the noise level, thus don't have a major impact in these measurements.

The minor errors observed could also be attributed to the fact that the values obtained from the photodiode were raw and unfiltered. Because of this, the photodiode measurements would sometimes deviate with a value of 1, instead of being constant. During

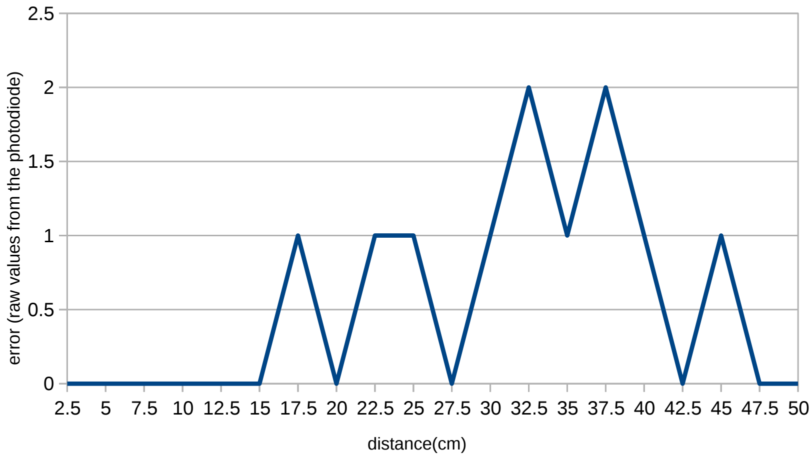

Figure 5.13: Errors in obtaining received power while modulation.

modulation, for each data frame, we consider 24 measurements from the photodiode, which increases the possibility for these errors.

However, these errors in received power do have an impact localization. Figure 5.14, shows the localization results for a modulating light source. We observed that localization errors were prominent when results from a modulated light source were compared with the benchmark results from a non-modulated light source in dark conditions (3 lux). The position estimates for a modulating light source at different illumination levels was found to be quite similar as expected. The average error in the x and y positions can be summarised in Table 5.1.

Table 5.1: Mean errors in X and Y positions while localization.

	Mean X position error (cm)	**Mean Y position error (cm)**
Non-Modulated Light source (3 lux)	1.45	2.08
Modulated Light Source (3 lux)	2.33	3.23
Modulated Light Source (200 lux)	2.91	3.55

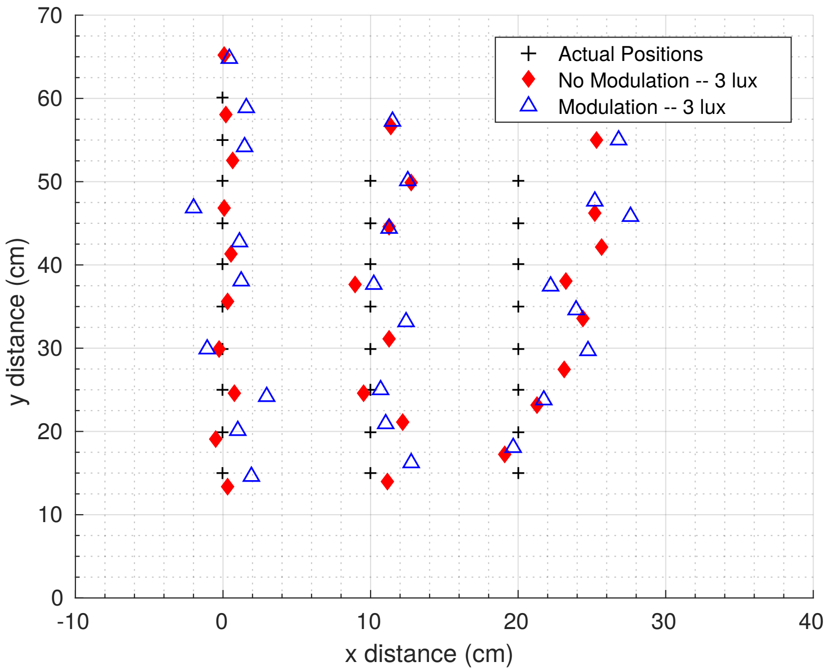

(a) Receiver positions with and without modulation

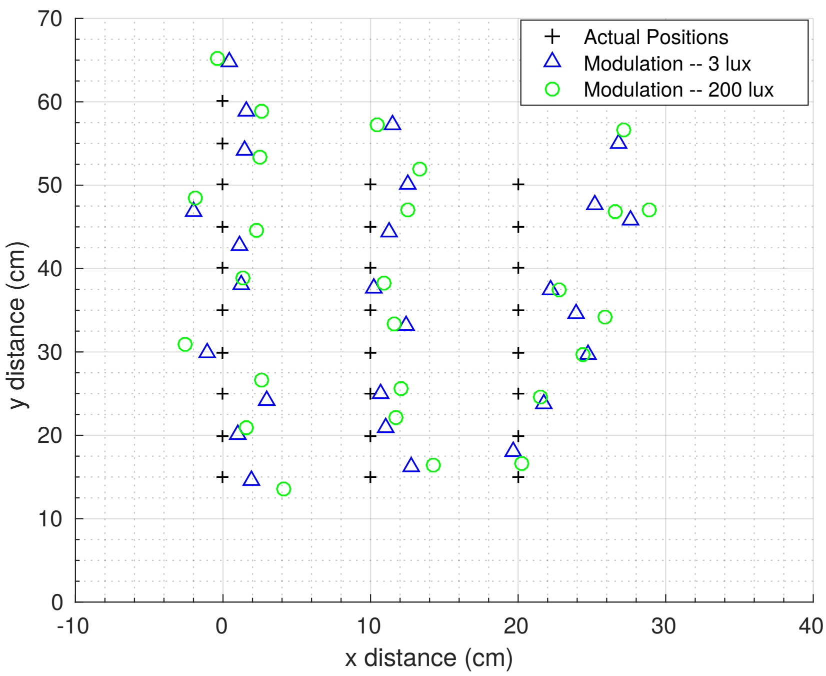

(b) Receiver postions using moduluation at diffrerent illumination levels

Figure 5.14: Localization while communication.

Analyzing Errors in Contours

As explained before, the location of a receiver is mainly derived from its orientation and the received power measured by it. These two things, are critical in deciding the shape of contours which are used for localization. Consequently, errors in measuring these values would reflect in the shape of the contours and eventually in the position of the node.

First, we analyse the effect of errors in received power. For this, a receiver was place at a distance of $30cm$ from the transmitter, with a relative angle of $0°$, i.e, both the Tx and Rx are aligned. For this state we obtain a contour of points where the receiver can be. Next, we simulate errors in received power while keeping the orientations of both the nodes constant. A similar experiment was conducted for analysing the effect of orientation errors on contour positions. The transmitter and receiver setup is the same as before, except now we change the orientation of the receiver while ensuring that the received power is constant. The maximum errors observed in the x and y positions of the contour points can be seen in figures 5.15 and 5.16.

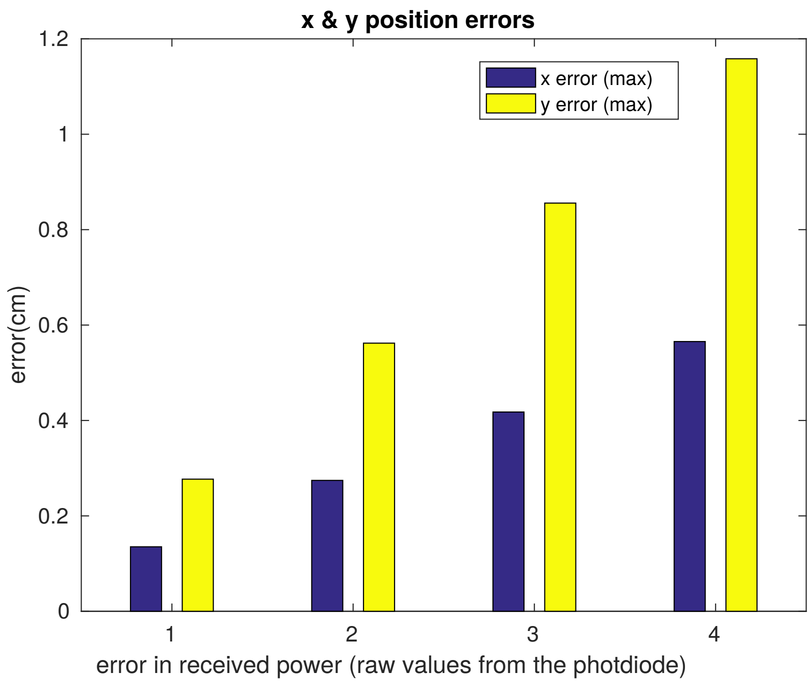

Figure 5.15: Maximum x & y position errors due to errors in received power.

We can see that there is a sharp increase in y-position errors compared to the x-position errors, when there are errors in received power. This is because, errors in received power *stretch or shrink* the contour along the y-axis. Whereas, errors due to orientation have larger impact on x-positions because, changes in orientation directly affect the irradiation angle, which in turn *shifts* this contour along the x-axis. This stretching and shifting of contours can be seen in Figure 5.17.

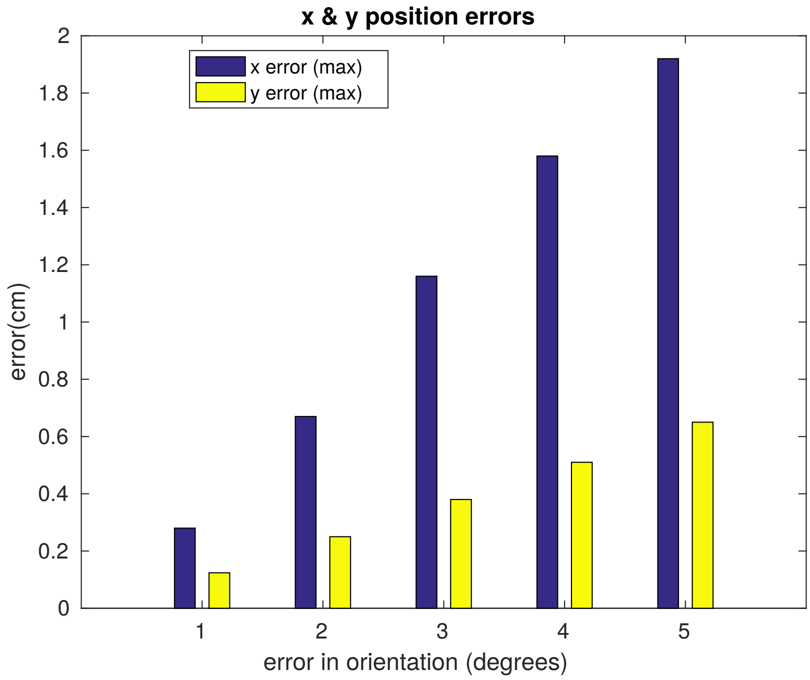

Figure 5.16: Maximum x & y position errors due to errors in orientation.

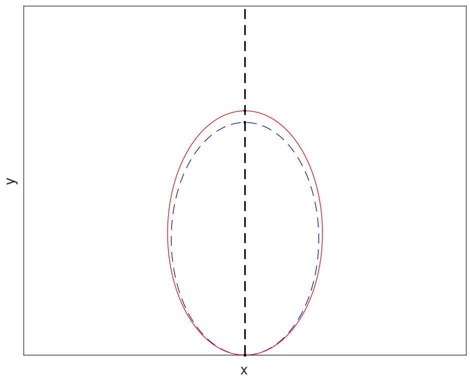

(a) Stretching contours along y axis due to errors in received power.

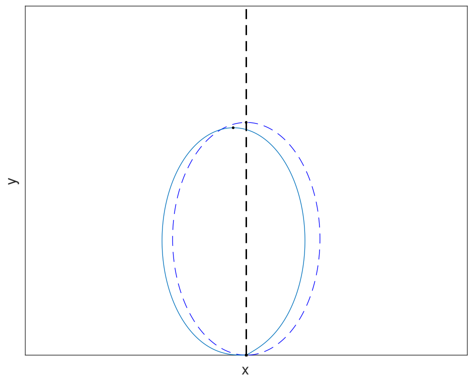

(b) Shifting contours along x-axis due to orientation errors

Figure 5.17: Stretching and shifting of contours.

5.2.2 Dynamic/mobile case

Unlike the static scenario, both nodes in this case are free to move and orient themselves in any direction. Orientation information and optical properties are shared between both nodes using visible light communication. We conducted experiments for this scenario, by moving both nodes on model tracks as shown in Figures 5.18 and 5.19 to simulate the movement of robots or vehicles on road. This was done by moving both nodes together on the track in an illuminated environment of 100 lux. Whenever, the node in *front* (transmitter in this case) was at a reference position shown in red, a measurement was taken. The location of the node *behind* (receiver), shown in blue is relative to these reference points. It must be noted that, for straight paths, like Track 1, ideally there should be no change in orientation of the nodes, however our localization model is based on changes in orientation. So for this experiment, we manually introduces minor changes in orientation, to obtain the position of the receiver.

One solution to this could be using an LED as a receiver. We mentioned earlier, that an LED can be used a receiver, but it is not very effective because of its limited field of view. However, this property can be advantageous in scenarios like Track 1, where a receiver just needs to know the position of a transmitter directly in front of itself.

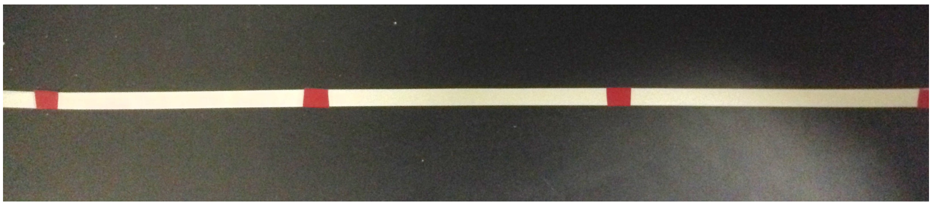

(a) Setup for Track 1

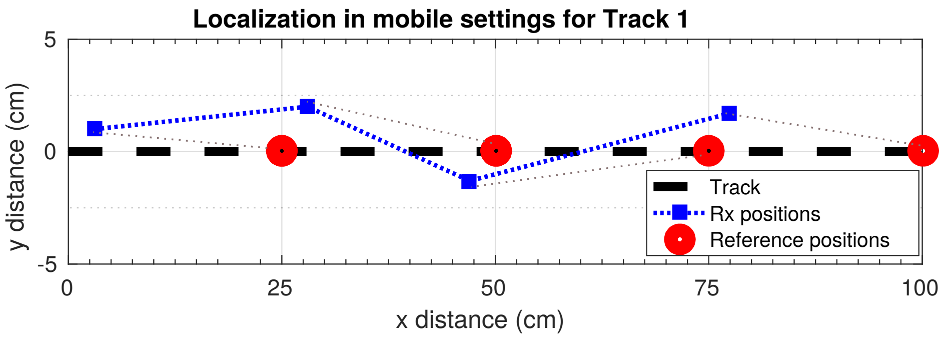

(b) Receiver postions for Track 1

Figure 5.18: Localization for Track 1.

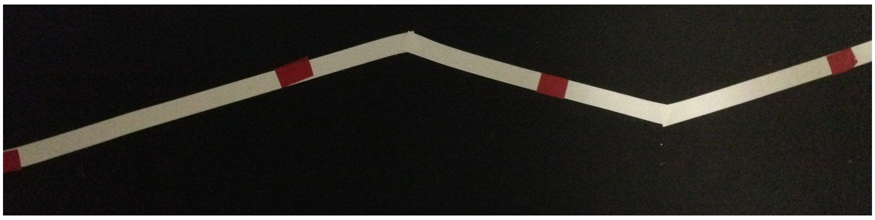

(a) Setup for Track 2

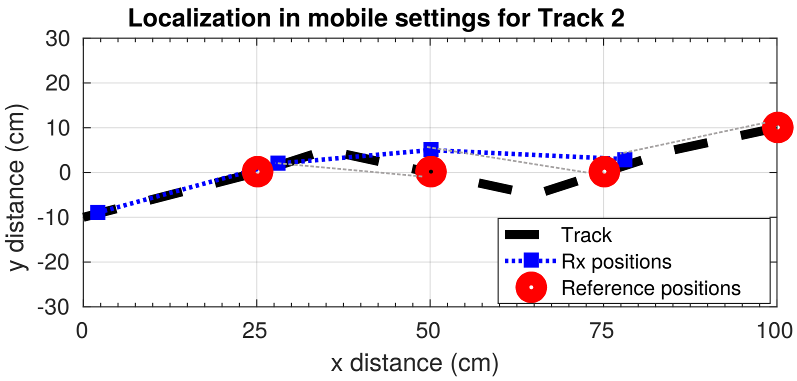

(b) Receiver postions for Track 2

Figure 5.19: Localization for Track 2.

5.2.3 Errors in orientation

To achieve localization in such dynamic environments, the orientation sensors of both the nodes should be well calibrated. In our experiments, the transmitter had an Android phone as an orientation sensor, whereas the receiver had a dedicated sensor BNO055 which used data from multiple sensors to give robust and resilient orientation information. It was observed that accurate localization was achieved as long as the orientation sensor from the Android phone was well calibrated. However, position errors were encountered when there were differences in orientations reported by both the nodes. Also, the orientation information, especially from the Android smartphone, was easily influenced by magnetic disturbances. These were caused due to nearby electronic devices, wires, and even the metal frame of the table on which experiments were performed.

A simple experiment was conducted for measuring the orientations reported by two nodes (two Smartphones in this case). The nodes were moved on a random path outdoors, away from any possible noise sources. The difference in the orientations reported by them can be seen in the Figure 5.20. From this figure we can see, that at some instances, there can be large differences in the orientations reported by both the nodes, which can have a significant impact on localization. Even though, a lot of these errors can be dealt with using filters, it would be suitable to obtain orientation information from a combination of sensors like gyroscope, magnetometer and accelerometer.

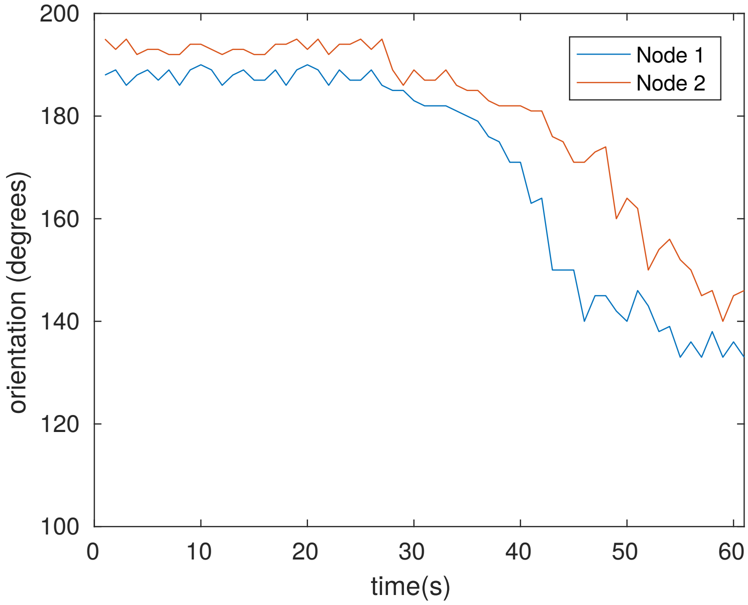

Figure 5.20: Orientations reported by two different nodes.

Chapter 6

Conclusions and Future Work

6.1 Conclusions

Localization based on visible light can be done accurately in mobile scenarios using considerably less infrastructure investment when compared to methods based on radio. Communication using visible light has shown great promise especially in the domain of Internet of Things. The existing lighting infrastructure seen in buildings, street lights and vehicles provide an excellent opportunity for localization. Using this as motivation, we have developed a localization model which can be used to find the relative position of objects using visible light. The model allows these objects or nodes in our proposed system to be mobile an independent of their environment. Moreover, the localization can be achieved using a minimal number of reference points, which in our case is as low as a single pair of transmitter and receiver. The proposed model has been described mathematically and validated experimentally to show high accuracy and mobility. Our evaluation also highlights the factors which affect the accuracy of this model.

6.2 Future Work

This work has helped us identify new opportunities for research. This model is based on a 2-D system, and thus it can be further extended to work in 3-D scenarios. One key challenge to tackle, would be to deploy the system in outdoor environments. For this sudden and severe changes in ambient light due to weather and surrounding buildings need to be dealt with. A possible solution can involve dynamically changing the light sensitivity of a receiver. Also, using an LED as a receiver in conjunction with this model could potentially improve its accuracy and robustness. Because an LED is a highly directional transmitter, it is also a directional receiver. Due to this it is more resilient towards bright sources of light and can prove to be useful in instances when a photodiode might saturate. Lastly, many different types of sensors can be used to retrieve orientation information. A comprehensive study/analysis is need to identify which sensor or a combination of sensors can be used to provide reliable and accurate information.

Bibliography

[1] Beagleboard.org - black. http://beagleboard.org/black. (Accessed on 13/09/2016).

[2] Openvlc. http://www.openvlc.org/home.html. (Accessed on 13/09/2016).

[3] Overview — bno055 absolute orientation sensor with raspberry pi & beaglebone black — adafruit learning system. https://learn.adafruit.com/bno055-absolute-orientation-sensor-with-raspberry-pi-and-beaglebone-black/overview. (Accessed on 20/09/2016).

[4] M. Z. Afgani, H. Haas, H. Elgala, and D. Knipp. Visible light communication using ofdm. In *2nd International Conference on Testbeds and Research Infrastructures for the Development of Networks and Communities, 2006. TRIDENTCOM 2006.*, pages 6 pp.–134, 2006.

[5] Ahmed Arafa, Sumant Dalmiya, Richard Klukas, and Jonathan F Holzman. Angle-of-arrival reception for optical wireless location technology. 23(6):1020–1023, 2015.

[6] Jean Armstrong, Y Ahmet Sekercioglu, and Adrian Neild. Visible Light Positioning : A Roadmap for International Standardization. (December):11–16, 2013.

[7] Christos Danakis, Mostafa Afgani, Gordon Povey, Ian Underwood, and Harald Haas. Using a CMOS Camera Sensor for Visible Light Communication. pages 1244–1248, 2012.

[8] Trong-Hop Do and Myungsik Yoo. An in-Depth Survey of Visible Light Communication Based Positioning Systems. *Sensors*, 16(5):678, 2016.

[9] Georg Kail, Patrick Maechler, Nicholas Preyss, and Andreas Burg. ROBUST ASYNCHRONOUS INDOOR LOCALIZATION USING LED LIGHTING. pages 1866–1870, 2014.

[10] Ye-Sheng Kuo, Pat Pannuto, Ko-Jen Hsiao, and Prabal Dutta. Luxapose: Indoor positioning with mobile phones and visible light. In *Proceedings of the 20th Annual International Conference on Mobile Computing and Networking*, MobiCom '14, pages 447–458, New York, NY, USA, 2014. ACM.

[11] Liqun Li, Pan Hu, Massachusetts Amherst, and Implementation Nsdi. Epsilon : A Visible Light Based Positioning System This paper is included in the Proceedings of the. *11th USENIX Symp. Netw. Syst. Des. Implement.*, (1):1–13, 2014.

[12] Hui Liu. Survey of Wireless Indoor Positioning\nTechniques and Systems. 37(6):1067–1080, 2007.

[13] Guoqiang Mao, Bar Fidan, and Brian D.O. Anderson. Wireless sensor network localization techniques. *Comput. Networks*, 51(10):2529–2553, 2007.

[14] Eric Monteiro, Steve Hranilovic, and Senior Member. Design and Implementation of Color-Shift Keying for Visible Light Communications. 32(10):2053–2060, 2014.

[15] S Rajagopal, R D Roberts, and Sang-Kyu Lim. IEEE 802.15.7 visible light communication: modulation schemes and dimming support. *Commun. Mag. IEEE*, 50(3):72–82, 2012.

[16] Richard Roberts, Praveen Gopalakrishnan, and Somya Rathi. Visible light positioning: Automotive use case. *2010 IEEE Veh. Netw. Conf. VNC 2010*, pages 309–314, 2010.

[17] Jayakorn Vongkulbhisal, Bhume Chantaramolee, Yan Zhao, and Waleed S. Mohammed. A fingerprinting-based indoor localization system using intensity modulation of light emitting diodes. *Microwave and Optical Technology Letters*, 54(5):1218–1227, 2012.

[18] Jelena Vučić, Christoph Kottke, Stefan Nerreter, Klaus-Dieter Langer, and Joachim W. Walewski. 513 mbit/s visible light communications link based on dmt-modulation of a white led. *J. Lightwave Technol.*, 28(24):3512–3518, Dec 2010.

[19] Qing Wang, Domenico Giustiniano, and Omprakash Gnawali. Low-cost, flexible and open platform for visible light communication networks. In *Proceedings of the 2Nd International Workshop on Hot Topics in Wireless*, HotWireless '15, pages 31–35, New York, NY, USA, 2015. ACM.

[20] Wikipedia. Inverse-square law — Wikipedia, the free encyclopedia. `http://en.wikipedia.org/w/index.php?title=Inverse-square%20law&oldid=738668591`, 2016. [Online; accessed 12-September-2016].

[21] Wikipedia. Photodiode — Wikipedia, the free encyclopedia. `http://en.wikipedia.org/w/index.php?title=Photodiode&oldid=724570825`, 2016. [Online; accessed 08-September-2016].

[22] Bo Xie, Shimin Gong, and Guang Tan. LiPro: light-based indoor positioning with rotating handheld devices. *Wirel. Networks*, 2016.

[23] Muhammad Yasir, Siu-Wai Ho, and Badri N Vellambi. Indoor Positioning System Using Visible Light and Accelerometer. *J. Light. Technol.*, 32(19):3306–3316, 2014.

[24] Liang Yin, Xiping Wu, and Harald Haas. Indoor visible light positioning with angle diversity transmitter. *2015 IEEE 82nd Veh. Technol. Conf. VTC Fall 2015 - Proc.*, 2016.

[25] S. Rajbhandari Z. Ghasemlooy, W. Popoola. *Optical Wireless Communications: System and channel modelling with MATLAB.*